energies

MDPI

Article

Optimal Design and Analysis of Sector-Coupled Energy System in Northeast Japan

Naoya Nagano, Rémi Delage and Toshihiko Nakata *

Department of Management Science and Technology, Graduate School of Engineering, Tohoku University, 6-6-11-815 Aramaki-Aza-Aoba, Aoba-ku, Sendai 980-8579, Japan; naoya.nagano.0930@gmail.com (N.N.); delage@tohoku.ac.jp (R.D.)

* Correspondence: nakata@tohoku.ac.jp; Tel.: +81-22-795-7004

Abstract: As for research on sector-coupled energy systems, few studies comprehensively deal with energy carriers and energy demand sectors. Moreover, few studies have analyzed energy conversion functions such as Power-to-Gas, Power-to-Heat, and Vehicle-to-Grid on the energy system performance. This study clarifies the required renewable resources and costs in the sector-coupled energy system and cost-optimal installed capacity and operation. We formulated an optimization model considering sector coupling and conducted a case study applying the model in the Tohoku region. As a result, due to sector coupling, the total primary energy supply (TPES) is expected to decrease, and system costs are expected to increase from 1.8 to 2.4 times the current level. System costs were minimized when maximizing the use of V2G by electric vehicles and district heating systems (DHS). From the hourly analysis, it becomes clear that the peak cut effect by Power-to-Heat and the peak shift effect by Vehicle-to-Grid result in leveling the output of electrolyzer and fuel synthesizer, which improves the capacity factor reducing capacity addition. Since a large amount of renewable energy is required to realize the designed energy system, it is necessary to reduce the energy demand mainly in the industrial sector. Besides, in order to reduce costs, it is required to utilize electric vehicles by V2G and provide policy support for district heating systems in Japan.

Keywords: energy system; sector coupling; power-to-gas; power-to-heat; vehicle-to-grid

Citation: Nagano, N.; Delage, R.; Nakata, T. Optimal Design and Analysis of Sector-Coupled Energy System in Northeast Japan. *Energies* **2021**, *14*, 2823. https://doi.org/10.3390/en14102823

Received: 25 March 2021
Accepted: 10 May 2021
Published: 14 May 2021

1. Introduction

The Paris Agreement was adopted in 2015, and it was agreed globally that CO_2 emissions would be reduced to zero by mid-century. It is essential to switch from a conventional fossil-fueled energy system to an innovative energy system with renewable energy resources. Many studies have been performed on integrating large amounts of renewables into energy systems in recent years, and many results have been reported. Lund et al. stated the need for smart energy systems that leverage the synergies of individual sectors to build the sustainable energy system at the lowest cost by consistently capturing energy systems [1]. Connolly et al. presented a scenario for a 100% renewable energy system in Europe in 2050, citing specific steps in terms of scientific and political certainty [2]. Niemi et al. also showed that the share of renewable energy in a region can be increased by considering energy interchange for multiple energy carriers [3]. The studies mentioned above provide suggestions on how to offset the intermittentness of volatile renewable energies and integrate them throughout the energy system. Based on these research results, Thellufsen et al. presented the concepts of "cross-border" and "cross-sector" and verified the effect [4]. As a result, both are important concepts, but it is stated that cross-sector-based system integration should be prioritized over cross-border-based transmission line enhancements. Syranidou et al. developed the transmission model with variable renewable energy sources (VRES) as main resources and applied it to integrate large-scale variable renewable energy sources in the future European power system [5].

"Cross-sector" is an approach for integrating energy systems by converting electricity to other energy carriers. In recent years, this concept has often been regarded as the term "sector coupling". Sector coupling is defined as the concept that promotes the use of variable renewable energy through system integration between electricity, heat, and transportation.

The coupling of electricity and synthetic fuels using hydrogen as an intermediate is generally called Power-to-Gas (P2G) and Power-to-Liquid (P2L). Various studies have been conducted on evaluating the manufacturing costs of synthetic fuels. Tremel et al. evaluated six types of synthetic fuels from the viewpoints of technology, economy, and acceptability [6]. Gotz et al. summarized the technical and economic barriers of electrolyzers, catalytic methanation, and biological methanation for P2G using renewable energy [7]. Guilera et al. showed that the technical and economic evaluation of SNG could reduce the cost of natural gas to the current cost level in the future [8]. These studies have had significant achievements in research and development by presenting the technical issues of synthetic fuels. However, since the role played by synthetic fuels differs depending on the application area and input conditions of the technology, research considering integration into the energy system is required. For instance, Ikaheimo et al. optimized plant capacity and operation in nine European countries with a model that integrates the power sector with synthetic fuel plants [9]. Varone et al. validated the contribution of P2L and P2G in the German energy system in 2050 in some scenarios of increased renewable energy introduction [10]. Blanco et al. analyzed 80–95% CO_2 reduction scenarios by 2050 (compared to 1990) to identify barriers and drivers of methanation [11]. Nastasi applied a solar Power-to-Gas system to an island energy system [12].

The coupling between electricity and heat is called Power-to-Heat (P2H), and there are many reports on the integration of electrical grid and heating systems. For instance, Bloess et al. simulated P2H and heat storage effects on the power sector by extending the long-term model of power development. As a result, P2H has been shown to increase electricity demand [13]. Obara et al. applied the optimization model that minimizes the system's economic efficiency to Hokkaido. As a result, it became clear that the system used was much cheaper than the storage battery. It was also confirmed that the introduction of renewable energy increased by 21.5% [14]. Ashfaq et al. used the model to examine the possibility of coupling the power grid and heating. The results suggest that current surplus electricity generation is not sufficient to support the heating sector fully, but heat storage can play an important role when renewable energy generation increases by 50% [15].

Vehicle-to-Grid (V2G), the system that utilizes battery electric vehicles as batteries for the electrical grid, is also the coupling between electricity and transportation. Many studies reported the impact of introducing V2G into the power system. For instance, Taljegard et al. simulated how the power supply mix changes with the spread of electric vehicles in Scandinavia and Germany. As a result, it was found that the V2G charging strategy for passenger car EVs smooths the net load curve and almost completely reduces the need for peak power capacity [16]. Child et al. analyzed a 100% renewable energy scenario by using EnergyPLAN. As a result, participation in V2G connectivity promoted a high share of variable RE on a daily and weekly basis [17].

These studies examine individual couplings in the energy system. However, incorporating multiple couplings may cause unanticipated effects because of differences in technical features, costs, and energy qualities. Therefore, research incorporating multiple couplings into the energy system is important for introducing renewable energy into the entire energy system. For instance, Brown et al. comprehensively analyzed cross-border and cross-sector synergies in Europe from electricity, heat, and transportation perspectives. As a result, it was shown that the cost reduction effect of sector coupling becomes weaker as the transmission line is strengthened. However, the energy demands of the industry are not considered in this study [18]. The industry occupies a large share of energy demand and is one of the consumers that has not yet fully introduced renewable energy. Therefore, it is necessary to analyze the amount of renewable energy introduced and the cost of the entire system required by sector coupling in the energy system that also considers industry.

Bailera et al. presented the review of Power-to-X processes as applied to the iron/steel industry [19]. In addition, since sector coupling is a concept for the overall optimization of the energy system, many stakeholders need to cooperate to manage the energy system. It is necessary to consider this cooperation method from the viewpoint of appropriate market management and the priority of technology introduction. However, so far, there has not been sufficient discussion about the optimal operation of each technology in the energy system and the role of individual couplings in Japan.

The purpose of this study is to clarify how much renewable energy is needed and how much it costs in a sector-coupled energy system (including industry) compared to the current situation in this country. We also clarify the cost-optimal installed capacity and operation of each technology. The present study provides useful knowledge for energy planning to realize decarbonization by clarifying the required technologies, their costs, and optimal operation. Among other technologies, sector coupling gives us another solution to lead a zero-carbon society having renewable energy resources. The study focuses on the Tohoku region in Northeast Japan, as it has more abundant renewable energy potential than other regions. Based on actual data on electricity and heat demand, we designed and analyzed a cost-effective energy system to show the benefits of introducing a sector coupling function replacing the conventional energy system. On 26 October 2020, the Prime Minister of Japan announced a carbon-neutral target for Japan by 2050. The newest policy upgraded Japan's previous long-term strategy of reducing emissions by 80% by 2050 to full decarbonization. The approach and results shown here could first contribute to a practical design for zero-carbon Japan toward 2050, making full use of domestic renewable resources.

First, the optimization model for designing sector-coupled energy systems is developed and applied to Japan's particular regional energy system. Then, some scenarios assuming decarbonized energy systems are analyzed using the model. Finally, the optimally designed energy systems' performances are compared, and each technology's optimal operations are explored.

In October 2020, the Government of Japan declared that it would aim to realize a decarbonized society by 2050. According to an IEA report [20], Japan's total primary energy supply (TPES) in 2017 was 18.01 EJ, of which about 93% depended on fossil fuels (including nuclear power). Furthermore, 93% of the total primary energy supply depends on imports from abroad. This is shown in the study on analyzing the energy flow and cash flow diagrams in Japan's energy system [21]. Therefore, expanding the introduction of renewable energy in Japan is a top priority from the environmental, economic, and energy security perspectives.

Furthermore, Japan is the country that emits the fifth largest amount of CO_2 in the world. If Japan manages to reduce most of its emissions, it would significantly impact the global environment and the international community. The implementation of decarbonized society plans by increasing transmission lines based on the cross-border concept is underway by the continued introduction of renewable energy in Japan. On the other hand, there is a description of "sector coupling" in the documents published by the Japanese Government and Ministries, but no detailed vision is drawn, and no research report has been made to support it. This research can be a primary material for examining sector coupling as one direction of Japanese future energy policy.

2. Methods

2.1. System Configuration of the Sector-Coupled Energy System

The energy system configuration with sector-coupling in this study is shown in Figure 1. Solar energy, wind energy, hydro energy, run-of-river, geothermal energy, and woody biomass are considered resources. Nuclear energy is not included as no nuclear power plants are in operation in the target area since the Great East Japan Earthquake of 2011. This model consists of five secondary energy carriers: electricity, hydrogen, synthetic fuels, high-temperature heat, and low-temperature heat. The conversion technologies

between carriers are electrolyzer, fuel cell (FC), fuel synthesizer (FS), heat-only boiler (HOB), combined heat and power (CHP), heat pump (HP), and electric boiler (EB).

Regarding the inputs and outputs of these conversion technologies, only the conversion of energy is considered, and the input of water to the electrolyzer is not considered in this model. Low-temperature waste heat from 60 to 80 °C is generated by the electrolyzer [22]. This waste heat was difficult to recover in the conventional district heating system (DHS) because of its low temperature. However, based on the concept of 4th generation district heating [23], heat recovery from electrolyzer is possible because the supply temperature can be lowered, and various heat resources can be used. Therefore, in this study, it is assumed that the electrolyzer's waste heat can be recovered. The fuel cell's waste heat can also be retrieved as low-temperature heat. As energy storage technology, stationary battery, hot water tank (HWT), high-pressure tank (HPT), and fuel tanks are handled in the model. If the heat source and heat demand are close to each other, heat storage can be considered, but this model does not reflect the location. Therefore, storage equipment of high-temperature heat is not handled in this research.

Synthetic fuels such as methane, methanol, dimethyl ether (DME), diesel, and gasoline can be produced by reacting hydrogen with CO_2 or CO. In this model, only CO_2 is considered a reactant for fuel synthesis, and they are supplied by direct air capture (DAC), biomass, and gas CHP plants. In the transportation demands, fuel cell vehicles (FCV) and battery electric vehicles (BEV) are taken into account because they do not emit exhaust gases such as CO_2 and NOx when running. The non-manufacturing industry consists of agriculture, forestry, fishery, construction, and mining. Therefore, fuels are mainly consumed by agricultural machines, forestry machines, fishing boats, and construction machines.

The remaining fuels are consumed in the manufacturing industry's heating process. Therefore, only synthetic fuel is supplied to the non-manufacturing industrial and high-temperature heat and synthetic fuels supplied to the industrial manufacturing sector. Local heat pumps are installed in customer's buildings. In the buildings connected to DHS, heat exchangers and radiators are installed.

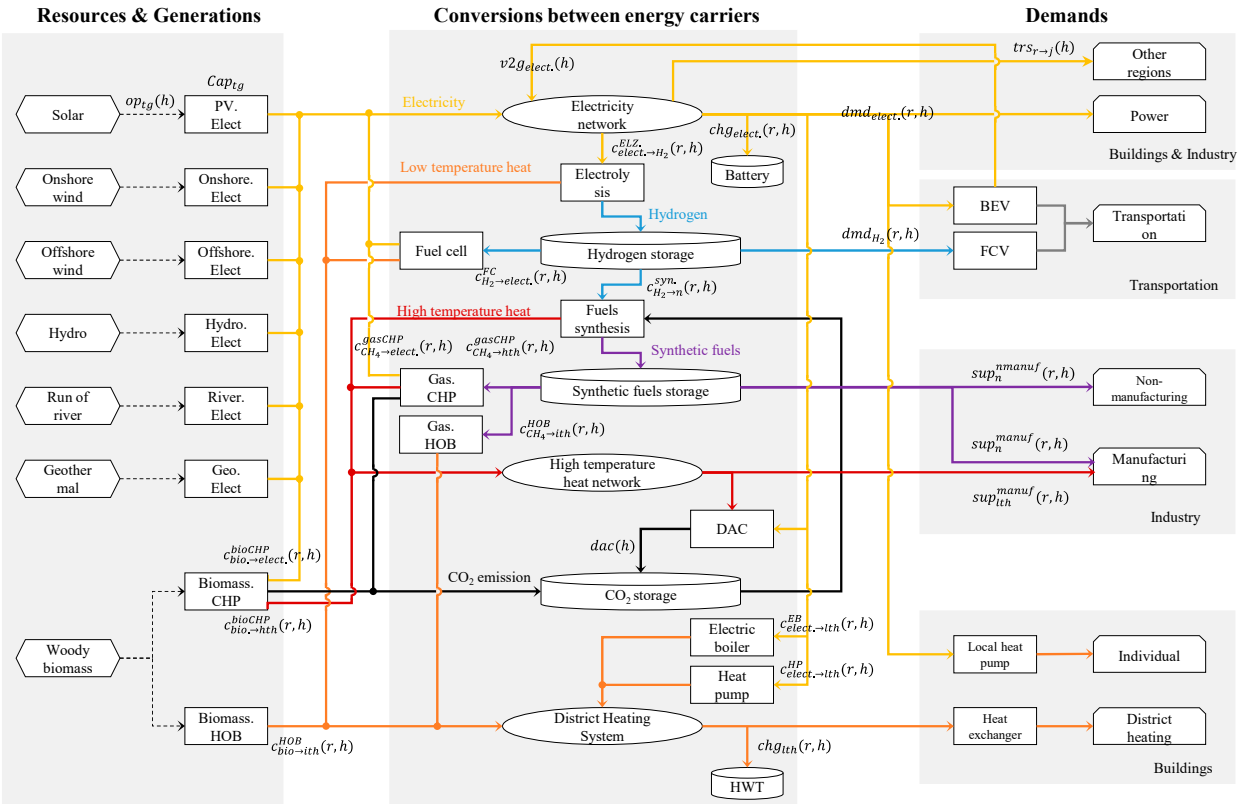

Figure 1. The system configuration of sector-coupled energy system designed in this study.

2.2. Optimization Model

This section describes the optimization model for designing sector-coupled energy systems. The proposed optimization model is formulated as a linear programming problem that minimizes the total annual system cost with each technology's installed capacity and the operations of these technologies as variables. The annual total system cost, which is the objective function, comprises capital, operation and maintenance costs, CO_2 procurement costs for fuel synthesis, costs for transmission between regions, and liquefaction cost of gaseous fuel as shown in Equations (1)–(10).

$$min.\ C^{total} = C^{CAPEX\&OPEX} + C^{carbon} + C^{trans.} + C^{liq.} \tag{1}$$

$$C^{CAPEX\&OPEX} = \sum_{r}\sum_{t} uc_{t}^{CAPEX\&OPEX} \cdot Cap_{t}(r) \tag{2}$$

$$C^{carbon} = uc_{bio.}^{cc} \cdot CC_{bio.} + uc_{gas}^{cc} \cdot CC_{gas} + uc_{DAC}^{cc} \cdot CC_{DAC} \tag{3}$$

$$C^{trans.} = uc^{trans.} \cdot \sum_{i}\sum_{h} trs(i,h), \tag{4}$$

$$C^{liq.} = uc^{liq.} \cdot \sum_{r}\sum_{h} liq_{CH_4}(r,h), \tag{5}$$

$$CC_{bio.} = \sum_{r}\sum_{h} \eta_{bio.}^{cc} \cdot cef_{bio.} \cdot pes_{bio.}^{bioCHP}(r,h), \tag{6}$$

$$CC_{CH_4} = \sum_{r}\sum_{h} \eta_{CH_4}^{cc} \cdot cef_{CH_4} \cdot pes_{CH_4}^{gasCHP}(r,h), \tag{7}$$

$$pes_{bio.}^{bioCHP}(r,h) = \frac{1}{\eta_{elect.}^{bioCHP}} \cdot \left\{ c_{bio.\to elect.}^{bioCHP}(r,h) + \xi^{bioCHP} \cdot c_{bio.\to hth}^{bioCHP}(r,h) \right\}, \tag{8}$$

$$pes_{CH_4}^{gasCHP}(r,h) = \frac{1}{\eta_{elect.}^{gasCHP}} \cdot \left\{ c_{CH_4\to elect.}^{gasCHP}(r,h) + \xi^{gasCHP} \cdot c_{CH_4\to hth}^{gasCHP}(r,h) \right\}, \tag{9}$$

$$CC_{DAC} = \sum_{r}\sum_{h} dac(r,h). \tag{10}$$

The first constraints are the hourly balances of electricity. In the electricity sector of region r, it is necessary to balance generation, transmission to other regions, conversion from other carriers, demand, conversion to other carriers, and charging of batteries with a time resolution of 1 h, as shown in Equation (11). The amount of electricity generation is calculated by adding up the product of installed capacity as a decision variable and the standardized output that depends on the time fluctuation of renewable energy resources as a given parameter for each generation technology as shown in Equation (12). The amount of electricity transmission is expressed as the sum of exports to other regions, which are decision variables. Here, the exports to other regions can take a negative value, which is an import (Equation (13)). The amount of conversion from other energy carriers to electricity is the sum of the amount of electricity generated by the fuel cell, biomass, and gas CHP, which are the decision variables (Equation (14)). The total electricity demand includes the amount of electricity required for DAC and methane liquefaction in addition to the local electricity demands (Equation (15)). The local electricity demands are given parameters, and the electricity required for DAC and methane liquefaction is calculated using the CO_2 captured from DAC and the amount of methane liquefied as decision variables. The amount of conversion from electricity to other energy carriers is the sum of the inputs of electricity to electric boilers and heat pumps in the DHS and electrolyzer, which are decision variables (Equation (16)).

Regarding charging, we distinguish between stationary and in-vehicle use. In this optimized model, the charging and discharging of batteries are represented by one variable. Therefore, in Equation (17), there are only two variables related to electricity storage. In the

case of a stationary battery, if the variable "*chg*" is positive, it means charging. In the case of in-vehicle use, if the variable "*v2g*" is positive, it means discharging.

$$G_{elect.}(r,h) + C'_{elect.}(r,h) = D_{elect.}(r,h) + C_{elect.}(r,h) + S_{elect.}(r,h) + T_{elect.}(r,h), \quad (11)$$

$$G_{elect.}(r,h) = \sum_{tg} Cap_{tg}(r) \cdot op_{tg}(r,h), \quad (12)$$

$$T_{elect.}(r,h) = \sum_{j} trs_{r \to j}(h), \quad (13)$$

$$C'_{elect.}(r,h) = \eta^{FC} \cdot c^{FC}_{H_2 \to elect.}(r,h) + c^{bioCHP}_{bio. \to elect.}(r,h) + c^{gasCHP}_{CH_4 \to elect.}(r,h), \quad (14)$$

$$D_{elect.}(r,h) = dmd_{elect.}(r,h) + er^{DAC}_{elect.} \cdot dac(r,h) + er^{liq.}_{elect.} \cdot liq(r,h), \quad (15)$$

$$C_{elect.}(r,h) = c^{ELZ.}_{elect. \to H_2}(r,h) + c^{EB}_{elect. \to lth}(r,h) + c^{HP}_{elect. \to lth}(r,h), \quad (16)$$

$$S_{elect.}(r,h) = chg_{elect.}(r,h) - v2g_{elect.}(r,h). \quad (17)$$

The amount of electricity stored in the batteries at a specific time is defined by adding the amount of charge to the amount of electricity stored 1 h ago, as shown in Equation (18). The amount of electricity storage is limited by the installed capacity of the stationary battery, which is a decision variable and its depth-of-discharge (DoD), which is assumed to be 80% in this model (Equation (19)). The maximum output of charging or discharging depends on the stationary battery's installed capacity (Equation (20)). The stored electricity in vehicles participating in V2G at time h is defined as shown in Equation (21). The amount of electricity stored in BEVs in the entire area is defined as the value obtained by subtracting the amount of electricity discharged to the grid and the electricity consumption due to running, a given parameter from the amount of electricity stored 1 h ago. The amount of electricity stored in vehicles is restricted by the storage capacity of the battery equipped in the vehicle and state of charge (SOC) (Equation (22)). The discharge to the grid is also limited by the number of inactive BEVs in the area, which is calculated from the given parameters as shown in Equation (24).

$$Sto^{battery}_{elect.}(r,h) = \left(1 - \eta^{battery}\right) \cdot Sto^{battery}_{elect.}(r,h-1) + chg_{elect.}(r,h), \quad (18)$$

$$\frac{1}{2} \cdot \left(1 - DoD^{battery}\right) \cdot Cap_{battery}(r) \le Sto^{battery}_{elect.}(r,h) \le \frac{1}{2} \cdot \left(1 + DoD^{battery}\right) \cdot Cap_{battery}(r), \quad (19)$$

$$-or^{battery} \cdot Cap_{battery}(r) \le chg_{elect.}(r,h) \le or^{battery} \cdot Cap_{battery}(r), \quad (20)$$

$$Sto^{bev}_{elect.}(r,h) = \left(1 - \eta^{battery}\right) \cdot Sto^{bev}_{elect.}(r,h-1) - v2g_{elect.}(r,h) - dmd^{transport.}_{elect.}(r,h), \quad (21)$$

$$SoC_{btm.} \cdot N_{vehicle}(r) \cdot cap_{vbattery} \le Sto^{bev}_{elect.}(r,h) \le SoC_{up} \cdot N_{vehicle}(r) \cdot cap_{vbatery}, \quad (22)$$

$$-V2GCap(r,h) \le v2g_{elect.}(r,h) \le V2GCap(r,h), \quad (23)$$

$$V2GCap(r,h) = \gamma \cdot \{1 - \alpha(r) \cdot \beta(r) \cdot p(r,h)\} \cdot N_{vehicle}(r) \cdot \theta^{vbattery}. \quad (24)$$

Low-temperature heat in DHS also needs to balance generation, conversion from other carriers, demand, and heat storage, as shown in Equation (25). The generation of low-temperature heat is defined as the amount of waste heat recovered from electrolyzers and fuel cells which are decision variables (Equation (26)). The conversion of other energy carriers to low-temperature heat is defined as the sum of the amount of heat supplied by each energy carrier to EB and HP in the DHS, and HOB of biomass and fuels, which are variables multiplied by the respective conversion efficiency (Equation (27)). The energy demand in DHS is defined as a given parameter which is the actual demand divided by the efficiency of the heat exchanger (Equation (28)). The amount of low-temperature heat stored in the hot water tank (HWT) at time h is defined by adding the amount of charge, which is a variable of the amount of low-temperature heat stored 1 h ago, as shown in

Equation (30), and is restricted by the installed capacity of HWT as a decision variable (Equation (31)).

$$G_{lth}(r,h) + C'_{lth}(r,h) = D_{lth}(r,h) + S_{lth}(r,h), \tag{25}$$

$$G_{lth}(r,h) = hr^{ELZ.}(r,h) + hr^{FC}(r,h), \tag{26}$$

$$\begin{aligned} C'_{lth}(r,h) = COP^{HP} \cdot c^{HP}_{elect.\to lth}(r,h) + \eta^{EB} \cdot c^{EB}_{elect.\to lth}(r,h) \\ + \eta^{HOB}_{CH_4} \cdot c^{HOB}_{CH_4\to lth}(r,h) + \eta^{HOB}_{bio.} \cdot c^{HOB}_{bio.\to lth}(r,h), \end{aligned} \tag{27}$$

$$D_{lth}(r,h) = \frac{1}{\eta^{HEX}} \cdot dmd_{lth}(r,h), \tag{28}$$

$$S_{lth}(r,h) = chg_{lth}(r,h), \tag{29}$$

$$Sto^{HWT}_{lth}(r,h) = \left(1 - \eta^{HWT}\right) \cdot Sto^{HWT}_{lth}(r,h-1) + chg_{lth}(r,h), \tag{30}$$

$$0 \le Sto^{HWT}_{lth}(r,h) \le Cap_{HWT}(r). \tag{31}$$

For high-temperature heat, heat production by CHP plants, waste heat during fuel synthesis, supply to the manufacturing industry, and heat demand for DAC must be balanced hourly as shown in (32). In the operation of CHP using woody biomass and synthetic methane, the output of electricity and the output of high-temperature heat satisfy (33)–(36).

$$c^{bioCHP}_{bio.\to hth}(r,h) + c^{gasCHP}_{CH_4\to hth}(r,h) + \eta^{hr} \cdot \sum_n \left(1 - \eta^{syn.}_n\right) \cdot c^{syn.}_{H_2\to n}(r,h) = sup^{manuf.}_{hth}(r,h) + er^{DAC}_{hth} \cdot dac(r,h),. \tag{32}$$

$$c^{bioCHP}_{bio.\to elect.}(r,h) \le Cap_{bioCHP}(r) + \xi^{bioCHP} \cdot c^{bioCHP}_{bio.\to hth}(r,h), \tag{33}$$

$$c^{bioCHP}_{bio.\to elect.}(r,h) \ge \sigma^{bioCHP} \cdot c^{bioCHP}_{bio.\to hth}(r,h), \tag{34}$$

$$c^{gasCHP}_{CH_4\to elect.}(r,h) \le Cap_{gasCHP}(r) + \xi^{gasCHP} \cdot c^{gasCHP}_{CH_4\to hth}(r,h), \tag{35}$$

$$c^{gasCHP}_{CH_4\to elect.}(r,h) \ge \sigma^{gasCHP} \cdot c^{gasCHP}_{CH_4\to hth}(r,h). \tag{36}$$

Hydrogen produced by the electrolyzer is stored in a high-pressure tank (HPT). The amount of hydrogen stored in the HPT is defined by the amount of hydrogen 1 h ago, the amount of hydrogen produced by the electrolyzer, and the amount of hydrogen required for fuel synthesis and FCV driving, which is a given parameter (Equation (37)). As shown in Equation (38), this storage amount should not exceed the installed capacity of HPT as a variable. If the production and consumption of hydrogen are always balanced, HPT is not installed. The electricity consumption of the compressor is not considered in this model. The storage amount of synthetic methane is defined as shown in Equation (39) based on the energy balance of the storage amount 1 h ago, and decision variables (methane production by methanation, consumption at CHP and HOB, supply to the industrial sector, and liquefaction volume) and is restricted by the installed capacity of the existing gas holder, which is a given parameter (Equation (40)). Synthesized methane in a gaseous state can be stored in a liquid state after liquefaction. At this time, electricity corresponding to the amount of liquefaction is consumed. The storage amount of methane in the liquid state is defined by Equation (41) and is restricted by the existing gas holder's installed capacity, which is a given parameter as shown in Equation (42). The storage amount of another synthetic fuel is defined as shown in Equation (43) based on the energy balance of the storage amount 1 h ago and decision variables such as fuel production by fuel synthesis, consumption at HOB, and supply to the industrial sector and is restricted by the installed capacity of existing storage technology, as shown in Equation (44).

$$Sto^{HPT}_{H_2}(r,h) = Sto^{HPT}_{H_2}(r,h-1) + \eta^{ELZ.} \cdot c^{ELZ.}_{elect.\to H_2}(r,h) - \sum_n c^{syn.}_{H_2\to n}(r,h) - c^{FC}_{H_2\to elect.}(r,h) - dmd_{H_2}(r,h), \tag{37}$$

$$0 \le Sto^{HPT}_{H_2}(r,h) \le Cap_{HPT}(r), \tag{38}$$

$$Sto^{tank}_{CH_4(g)}(r,h) = Sto^{tank}_{CH_4(g)}(r,h-1) + \eta^{MTN.}\cdot c^{MTN.}_{H_2\to CH_4}(r,h) - pes^{gasCHP}_{CH_4}(r,h) - sup^{nmanuf.}_{CH_4}(r,h) - sup^{manuf.}_{CH_4}(r,h) - c^{HOB}_{CH_4\to lth}(r,h) - liq_{CH_4}(r,h), \quad (39)$$

$$0 \le Sto^{tank}_{CH_4(g)}(r,h) \le Cap_{gastank}(r), \quad (40)$$

$$Sto^{tank}_{CH_4(l)}(r,h) = Sto^{tank}_{CH_4(l)}(r,h-1) + liq_{CH_4}(r,h), \quad (41)$$

$$0 \le Sto^{tank}_{CH_4(l)}(r,h) \le Cap_{gasholder}(r), \quad (42)$$

$$Sto^{tank}_{n}(r,h) = Sto^{tank}_{n}(r,h-1) + \eta^{syn.}\cdot c^{syn.}_{n}(r,h) - sup^{nmanuf.}_{n}(r,h) - sup^{manuf.}_{n}(r,h) - c^{nHOB}_{n}(r,h), \quad (43)$$

$$0 \le Sto^{tank}_{n}(r,h) \le Cap_{ntank}(r). \quad (44)$$

The stock of woody biomass starts with the annual potential for use, and the stock decreases with the use of CHP and HOB, as shown in Equations (45)–(47). The storage of CO_2 is defined as in Equation (48) based on the balance of storage 1 h ago, the CO_2 recovery from CHP, and the CO_2 demand for fuel synthesis. The amount of CO_2 stored should not exceed the capacity of the introduced CO_2 tank, as shown in Equation (49).

$$Sto_{bio.}(r,h) = Sto_{bio.}(r,h-1) - pes^{bioCHP}_{bio.}(r,h) - c^{HOB}_{bio.\to lth}(r,h), \quad (45)$$

$$Sto_{bio.}(r,1) = Pot_{bio.}(r), \quad (46)$$

$$Sto_{bio.}(r,h) \ge 0, \quad (47)$$

$$Sto_{CO_2}(r,h) = Sto_{CO_2}(r,h-1) + dac(r,h) + \eta^{cc}_{bio.}\cdot cef_{bio.}\cdot pes^{bioCHP}_{bio.}(r,h) + \eta^{cc}_{CH_4}\cdot cef_{CH_4}\cdot pes^{gasCHP}_{CH_4}(r,h) - \sum_n cd_n\cdot c^{syn.}_{H_2\to n}(r,h), \quad (48)$$

$$0 \le Sto_{CO_2}(r,h) \le Cap_{CO_2tank}. \quad (49)$$

The fuel consumption of the industrial sector is not captured every hour. In addition, many consumers often have storage facilities. Therefore, in this model, the fuel supply-demand balance in the industrial sector is satisfied in 1 year. Agriculture, forestry and fisheries, and construction are the main consumers in the non-manufacturing industry. Agricultural machinery and construction machinery account for a large proportion, making it difficult to supply energy with high-temperature heat or gas. Therefore, the current city gas is replaced with synthetic methane, gasoline/light oil is replaced with methanol, and LPG is replaced with DME in this model. This is defined by Equation (50). Since fuel consumption in the manufacturing industry is ultimately supplied as process heat, it is considered that most of the fuel is used for combustion, and no distinction is made, as shown in Equation (51).

$$\sum_h sup^{nmanuf.}_{n}(r,h) = dmd^{nmanuf.}_{n}(r), \quad (50)$$

$$\sum_h \left\{ sup^{maunf.}_{hth}(r,h) + \sum_n sup^{manuf.}_{n}(r,h) \right\} = dmd^{manuf.}(r). \quad (51)$$

The installed capacity of generation technology, which is a decision variable, is limited by the introduction potential considering the restrictions on land use, etc., as shown in Equation (52). The outputs from conversion technologies at each time must not exceed the

installed capacity (Equation (53)). The transmission line between regions is restricted not to exceed the transmission line's capacity, as shown in Equation (54).

$$0 \leq Cap_{tg}(r) \leq Pot_{tg}(r), \tag{52}$$

$$0 \leq c^{tc}(r,h) \leq Cap_{tc}(r), \tag{53}$$

$$-Cap_{trs.}(i) \leq trs(i,h) \leq Cap_{trs.}(i). \tag{54}$$

2.3. Input Data and Assumptions

2.3.1. Target Region

In this study, the Tohoku region of Japan is considered a target region because the renewable resources potential is sufficient to give the optimization model feasible solutions. This region is located in the northeastern part of Japan and consists of Aomori, Akita, Iwate, Miyagi, Yamagata, Fukushima, and Niigata prefectures. These seven prefectures are defined as "regions" in the optimization model. The Tohoku region has 79,531 km^2 and a population of 11.28 million. In other words, 9% of the population resides in 21% of Japan's area. The spatial characters of energy supply and demand in the Tohoku region are shown in Figure 2. Figure 2a–c show the estimation results applying methods described later in Sections 2.3.2 and 2.3.3. Energy demand is high in the southern regions such as Miyagi, Niigata, and Fukushima. Renewable energy potential is estimated by considering the capacity factor of each technology. Tohoku region has much potential for offshore wind, particularly in Aomori and Akita. This is because offshore wind power's capacity utilization rate is high in these regions, leading to a reduction in the power generation cost of offshore wind power. The grid is modeled considering the capacity of significant transmission lines [24,25] in the Tohoku region, as shown in Figure 2d. Since the Tohoku region is connected to the other areas by inter-regional transmission lines, it can transmit these regions. However, this study does not consider transmission to the other regions. The transmission cost is assumed to be 4.5 JPY/kWh per link [26].

2.3.2. Estimation of Energy Demands

For estimating the hourly electricity demand in each region, the actual data are referenced [27]. Since these data are the demand for the entire target area, it is prorated by the annual data [28] for each of the seven prefectures. Low-temperature heat demand is defined as the demand for space and water heating in residential and commercial sectors. In this study, the low-temperature heat demand in the target area is estimated based on spatial information analysis. The residential sector's annual heat demand is calculated from households [29] and the annual heat demand per household [30]. That of the commercial sector is estimated using the same method as Fujii et al. [31]. This method estimates annual heat demand from the total floor area [32] and the heat demand intensity of each business.

Furthermore, the hourly heat load is estimated from the above heat demand and the daily heat load patterns [33] for each month. These patterns are categorized by household and business. Some of the estimated heat demand has already been electrified. Therefore, electrified heat demand is deducted from electricity demand. Figure 2c shows the spatial distribution of heat demand in the Tohoku region. When designing power and heat coupling, it is desirable to use existing DHSs to reduce capital costs. However, there are very few DHSs in the target area. In addition, these systems are small-scale systems with a small number of consumers. Therefore, it is necessary to estimate the capital cost of distribution networks if new DHSs are installed in this region. This "distribution capital cost" of DHS is obtained from the heat-demand density and spatial information [34].

Transportation demands are classified into passengers and freights. Each annual mileage is referenced from the statistics on traffic [35]. Annual transportation fuel demand is estimated by multiplying this mileage by each vehicle's tank-to-wheel efficiency. The tank-to-wheel efficiency is summarized in Table 1 [36–38]. The hourly energy demand for FCV and BEV is assumed to occur when the energy is charged, not during driving. Energy consumption not related to driving, such as air conditioning in a car, is not considered. The amount of filling per hour is referenced from the database on charging electric vehicles [39].

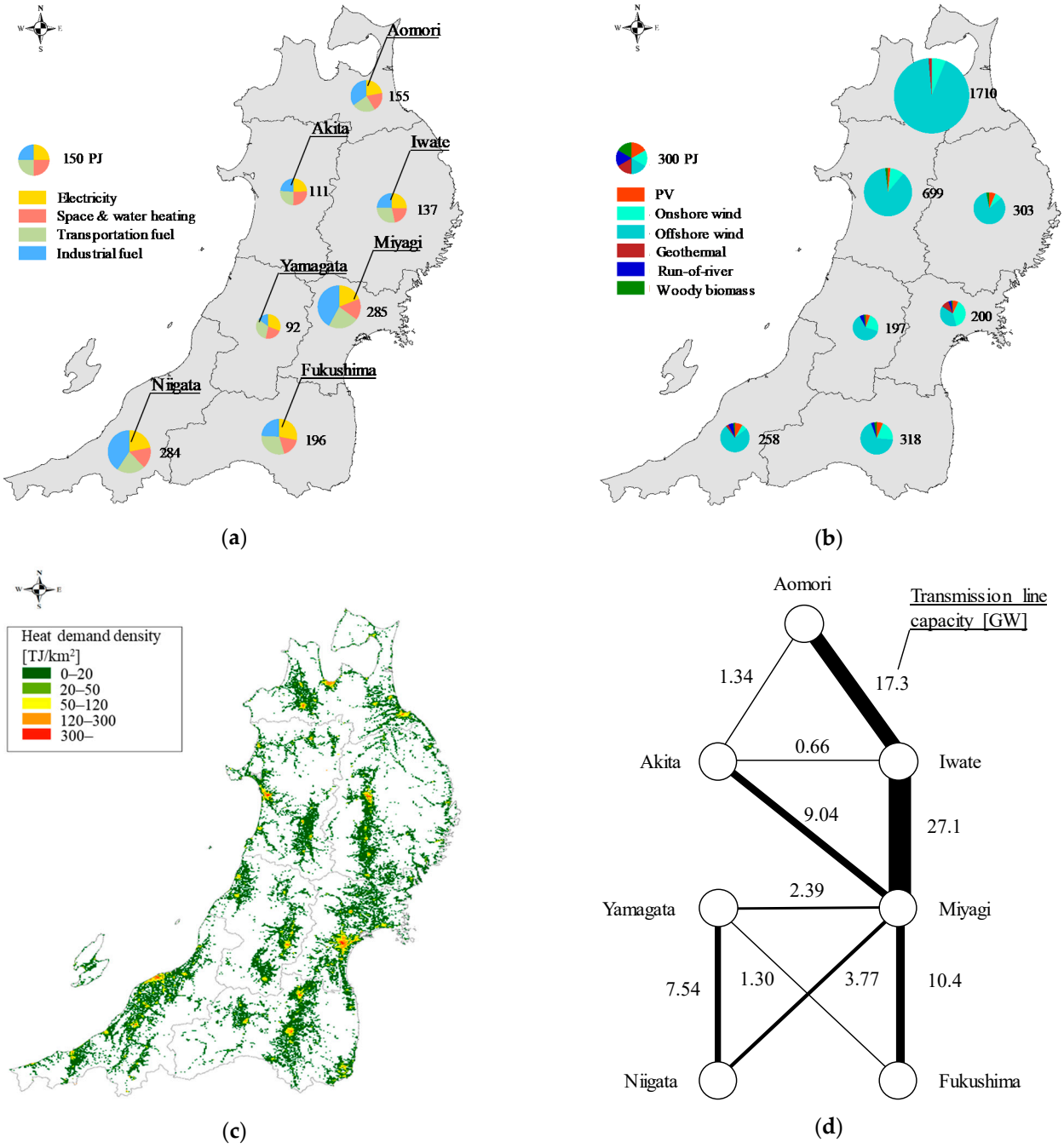

Figure 2. Spatial information of energy system in Tohoku region. (**a**) Energy demands. (**b**) Renewable energy potential. (**c**) Heat demand density map. (**d**) Modeled electrical grid.

Table 1. Tank-to-wheel efficiency of each type of vehicle [kWh/km].

		BEV	FCV
Passenger	Standard-sized	0.16	0.30
	Large-sized	1.19	3.54
Freight	Standard-sized	0.16	0.30
	Large-sized	2.09	3.00

The fuel demands for industrial use in each region are referenced from statistics on energy demand in each prefecture [28]. In addition to the energy demands mentioned above, there are energy demands for cooking and cooling use in the residential and commercial sectors. These energy demands are partially electrified, but many are still filled with fossil fuels. For exhaustive analysis, it is necessary to consider the electrification of these energy demands. However, it is difficult to estimate its hourly demand accurately, and the proportion of the total consumption is tiny. Therefore, the energy demands that are not electrified are excluded from the analysis. Energy demands for ships, railways, and aircraft in the transport sector are also excluded from the study because it is difficult to distinguish between specific regions.

2.3.3. Estimation of Energy Supply from Renewable Energy

As the upper limit on renewable generation technology has installed capacity in the optimization model, the introduction potential is referenced [40]. The hourly output standardized by the installed capacity from PV and wind turbine is estimated from the sample year's weather data. First, the standardized output of PV is calculated from Equation (55). The amount of solar radiation is referenced from meteorological data at an observation point in each prefecture [41]. Other technical parameters of PV are referenced from a product catalog [42].

$$op_{PV}(r,h) = \frac{1}{3.6} \cdot rad(r,h) \cdot A \cdot \eta_{panel} \cdot \eta_{pc}. \quad (55)$$

The standardized output of wind power generators is estimated by the same method as Obara et al. [14]. The wind speed at the ground level at the observation point is converted to the wind speed at the hub height, and this wind speed is substituted into the wind turbine's output curve. Cut-in wind speed is 2.5 m/s, rated wind speed is 12.5 m/s, and cut-out wind speed is 25.0 m/s. The wind speed at all observation points in each prefecture [41] is referenced for estimating the output of onshore wind power generators. The wind speed at the cape in each prefecture [43] is referenced to calculate offshore wind power generation's output.

The standardized output from geothermal is obtained by dividing the power company's actual data by the current geothermal power generation capacity. As for hydropower generation, it is assumed that the existing power plant is maintained in light of the situation where no further expansion is expected in Japan. The generation from run-of-river is considered to have a constant output at a load factor of 60%. The biomass resource optimized by the model is limited to woody biomass. It is assumed that the woody biomass resource that can be supplied per year is the annual stand growth volume [44].

2.3.4. Technical and Economic Parameters

Table 2 summarizes the model's technologies and its technical and economic parameters. The annual unit cost of technology t is calculated (Equations (56)–(58)), considering the overnight cost, operation and maintenance cost, lifetime, and efficiency, in Table 2. The interest rate I is assumed to be uniformly 2%. In this study, the target synthetic fuels are methane, methanol, and DME. This is because the synthesis of gasoline and diesel oil is costly and has a lower conversion efficiency [45]; therefore, there is no opportunity to introduce it by optimization. In this model, the introduction cost of energy conversion

equipment in the customer is not considered; therefore, the introduction cost of local heat pump, heat exchanger, FCV, and BEV is ignored.

Table 2. Technical and economic parameters in the optimization model.

	Unit	Overnight Cost [JPY]	Fixed O&M Cost [JPY/year]	Lifetime [year]	η [-]	References
Solar PV	kW_{el}	294,000	6000.0	25	1.00	[46]
Onshore wind	kW_{el}	300,000	6000.0	25	1.00	[46]
Offshore wind	kW_{el}	565,000	22,500.0	25	1.00	[46]
Run-of-river	kW_{el}	1,000,000	171,590.9	22	1.00	[46]
Biomass-CHP (CCS)	kW_{el}	250,000	7125.0	40	0.35	[47,48]
Gas-CHP (CCS)	kW_{el}	112,500	3750.0	25	0.47	[47,48]
Geothermal	kW_{el}	790,000	33,000.0	15	1.00	[46]
Battery (Li-ion)	kWh	68,250	862.5	15	0.95	[49]
Biomass-HOB	kW_{th}	100,000	7125.0	20	1.08	[47]
Hot water tank	kWh	1125	0.0	30	0.95	[13]
Heat pump in DHS	kW_{th}	87,500	250.0	25	4.50	[47,50]
Electric boiler	kW_{th}	8750	137.5	20	0.98	[47]
Gas-HOB	kW_{th}	7500	250.0	25	1.03	[47]
Electrolyzer (PEM)	kW_{el}	232,500	11,625.0	20	0.62	[45,51]
High pressured tank	kWh	16,250	0.0	20	1.00	[49]
Fuel cell	kW_{el}	405,375	3125.0	20	0.42	[49]
Methanation	kW_{fuel}	75,000	3000.0	25	0.77	[45]
Methanol synthesis	kW_{fuel}	125,000	5000.0	25	0.79	[45]
DME synthesis	kW_{fuel}	125,000	5000.0	25	0.80	[45]
Methane liquefaction	kW_{fuel}	9533	0.0	25	1.00	[52]
Direct Air Capture	tCO_2/year	28,500	1140.0	30		[53]
CO_2 tank	tCO_2	225,000	0.0	20	1.00	[9]

Similarly, the introduction cost of filling facilities that supply energy to FCVs and BEVs is not considered. The efficiencies of solar PV, onshore wind, offshore wind, run-of-river, and geothermal are 1.00 because those resources are not depleting and utilize some of the almost inexhaustible energy. The efficiencies of biomass-CHP and gas-CHP in Table 2 are electrical efficiency. The efficiency of the fuel cell in Table 2 is also electrical efficiency. The thermal efficiency of HOB exceeds 1 because it is calculated using the lower calorific value.

$$uc_t^{CAPEX\&OPEX} = uc_t^{capital} + uc_t^{O\&M} + uc_t^{fuel}, \tag{56}$$

$$uc_t^{capital} = c_t^{overnight} \cdot CRF_t, \tag{57}$$

$$CRF_t = \frac{I \cdot (1+I)^{Life_t}}{(1+I)^{Life_t} - 1}. \tag{58}$$

It assumes an air heat source heat pump as a local heat pump in commercial and residential sectors. The local heat pump's coefficient of performance (COP) is affected by the ambient temperature and the supply temperature [54]. In this analysis, the supply temperature is assumed to be 60 °C. The heat exchange efficiency in buildings connected to the DHS is 80%. The value of output ratio of stationary battery is 0.22 [kw/kWh]. It was set from the cost per output [Euro/kW] and the cost per capacity [Euro/kWh]. The vehicle's battery capacity and electricity output for V2G is assumed to be 62 kWh for battery capacity and 6 kW for output [55]. SOC of batteries in vehicles that participate in V2G is between 30% and 90% to maintain the batteries' life cycle within an acceptable range [56].

It is assumed that the fuel cost of woody biomass is 12,750 JPY/t, and the unit calorific value is 15 MJ/kg [46]. The energy consumption for transporting woody biomass is not taken into account. The cost of biomass resources supplied to the construction industry, pulp, and paper industry, wood product manufacturing industry, etc., within current statistics is not evaluated. The heat recovery efficiency from the electrolyzer and fuel synthesis

is assumed to be 90%. It is assumed that CO_2 captured by DAC requires 225 kWh/t-CO_2 of electricity and 1500 kWh/t-CO_2 of high-temperature heat [53]. CO_2 capture cost by DAC is assumed to be 2594 JPY/t-CO_2 [53]. The steam turbine is assumed to be the prime mover of the biomass CHP, and the gas turbine is assumed to be the prime mover of the gas CHP. Assuming that the energy required for CO_2 capture from the CHP plant is produced in the plant, it can be expressed by a decrease in energy conversion efficiency. According to [48], it was shown that the power generation efficiency of coal-fired power plants that capture CO_2 is reduced by 23%, compared to the case without capture.

Therefore, it is assumed that the efficiency of the biomass plant is also reduced by 23% from the efficiency without CO_2 capture, which is 46%. For gas CHP plants, efficiency is reported to decrease by 14%. The CO_2 capture efficiency is assumed to be 90%. The CO_2 emission factors for biomass and methane are considered to be 98.7 kg-CO_2/MJ [57] and 51.1 kg-CO_2/MJ [58], respectively. The capture costs are also assumed to be 5060 JPY/t-CO_2 and 8140 JPY/t-CO_2, respectively [48]. It is assumed that synthetic fuels' storage facilities are already in use. In this case, the capital cost of the storage facility is ignored. The storage capacity of methane, methanol, and DME is referenced from [59,60].

3. Results

3.1. Scenario Setting

Table 3 summarizes the scenarios in this study. There are three scenarios on transportation demands. As with the report by U. Persson et al. [61], heat demand is classified into areas of 120 TJ/km^2 or less, 120–300 TJ/km^2 (dense heat density class), and 300 TJ/km^2 or more (very thick heat density class) according to the heat-demand density. Individual or district heating is provided to each of these areas. There are three scenarios on heat demands.

Table 3. Description of scenarios analyzed in this study.

Scenarios	Definition
	Transportation
All-FCV	All transportation is provided by fuel cell vehicles.
All-BEV	All transportation is provided by battery electric vehicles.
All-BEV-V2G	All transportation is provided by battery electric vehicles, and the normal-sized vehicle can be used for vehicle-to-grid.
	Heat demand
IND	All heat demand is met by individual heating.
HD300	DHS is introduced in areas where the heat-demand density is over 300 TJ/km^2
HD120	DHS is introduced in areas where the heat-demand density is over 120 TJ/km^2

3.2. Comparison of Total Primary Energy Supply (TPES) and Total Annual System Cost in Each Scenario

Figure 3a shows the configuration of the primary energy supply of each scenario based on the results of the optimization calculation. TPES is estimated by Equation (59). TPES in the current energy system is estimated using statistics [28], not using the proposed model. Compared with the current, TPES decreases in almost all scenarios because of the reduction of heat loss at the existing thermal power plants, the improvements of tank-to-wheel efficiency by a shift to BEV and FCV, and the improvements of energy efficiency to produce heat in commercial and residential sectors. TPES of All-FCV scenarios are larger than that of All-BEV and All-BEV+V2G scenarios because the tank-to-wheel efficiency of FCV is lower. There is no significant difference in TPES between All-BEV and All-BEV-V2G scenarios. TPES of HD300 and HD120 scenarios tend to increase slightly compared to IND scenarios because of the difference in efficiency between the heat exchanger and local HP in consumers. Offshore wind accounts for more than 70% of the total primary energy supply

in all scenarios. The primary energy supply of solar tends to increase in the scenarios in which DHS is introduced.

$$TPES = \sum_{r}\sum_{h}\left\{\sum_{tg} Cap_{tg}(r)\cdot op_{tg}(r,h) + pes_{bio.}^{bioCHP}(r,h) + c_{bio.\rightarrow lth}^{HOB}(r,h)\right\} \quad (59)$$

Figure 3b shows the breakdown of the total annual system cost, the optimization model's objective function. Regarding the total annual system cost in the current energy system, the generation cost is estimated from the power generation amount and generation unit price [JPY/kWh] (including capital cost and O&M cost) of each technology, and the fuel cost is estimated from the primary energy supply amount and wholesale unit price of each fuel, not from the proposed model [46,58]. As a result, the current energy system's total annual system cost was 4079.7 billion JPY/year. The total annual system cost increases from 80% to 140% of the current system cost. All-BEV scenarios' annual total system cost was lower than that of all-FCV scenarios because all-FCV scenarios' total primary energy supply is larger. The whole system cost of All-BEV-V2G scenarios is reduced by about 10% compared to all-BEV scenarios. The capital and O&M costs of CHP, electrolyzer, and stationary storage battery are mainly reduced by introducing V2G. Comparing IND scenarios with HD300 and HD120 scenarios, the DHS's introduction reduced the total system cost. The distribution cost in DHS and capital and O&M costs of heat source equipment and heat storage tanks are less than 1% of the entire system cost. Compared to IND scenarios, the cost of electricity generation tends to increase. However, the total system costs are decreased since the cost reduction of stationary storage batteries and electrolyzers exceeds the increase.

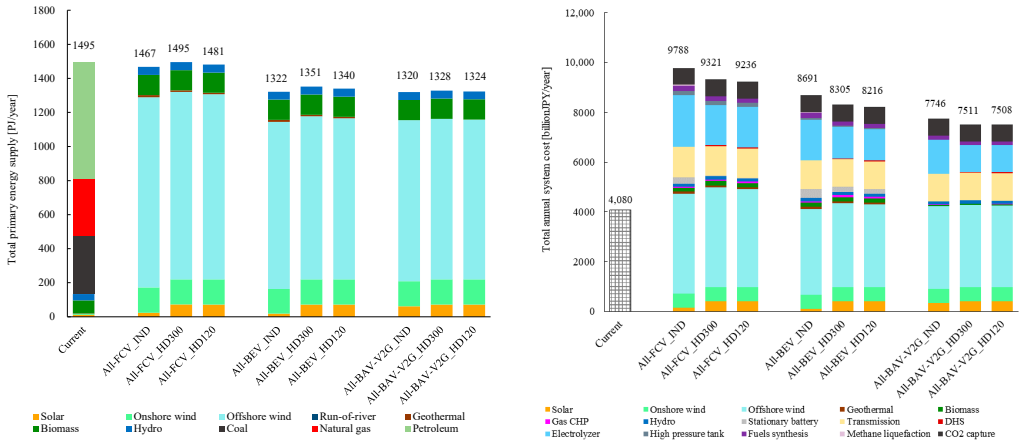

(**a**) (**b**)

Figure 3. Comparison of system performance in each scenario. (**a**) TPES. (**b**) Total annual system cost.

3.3. Installed Capacity of Each Technology

This section shows the solved installed capacity, a variable of the total annual system cost. All-BEV_IND, All-BEV_HD120, All-BEV-V2G_IND, and All-BEV-V2G_HD120 scenarios are compared. The installed capacity of each technology is shown in Figure 4. The installed capacity of offshore wind generation in Aomori, Akita, and Niigata prefectures tends to be large. Miyagi and Yamagata prefectures have a large percentage of installed solar PV and onshore wind generation capacity. No generation technology is installed in Iwate. This result is explained by the relationship between the levelized cost of electricity (LCOE) of each generation technology and the transmission costs between regions. A generation technology in a specific region is installed at a lower price than the LCOE in the region and the LCOE in the other region, considering the transmission cost. For example, the offshore wind LCOE in Aomori Prefecture is 9.9 JPY/kWh. If this electricity is consumed in Niigata Prefecture, its actual cost would be 24.4 JPY/kWh. In other

words, LCOE for different generation technologies in Niigata is cheaper than offshore wind power in Aomori.

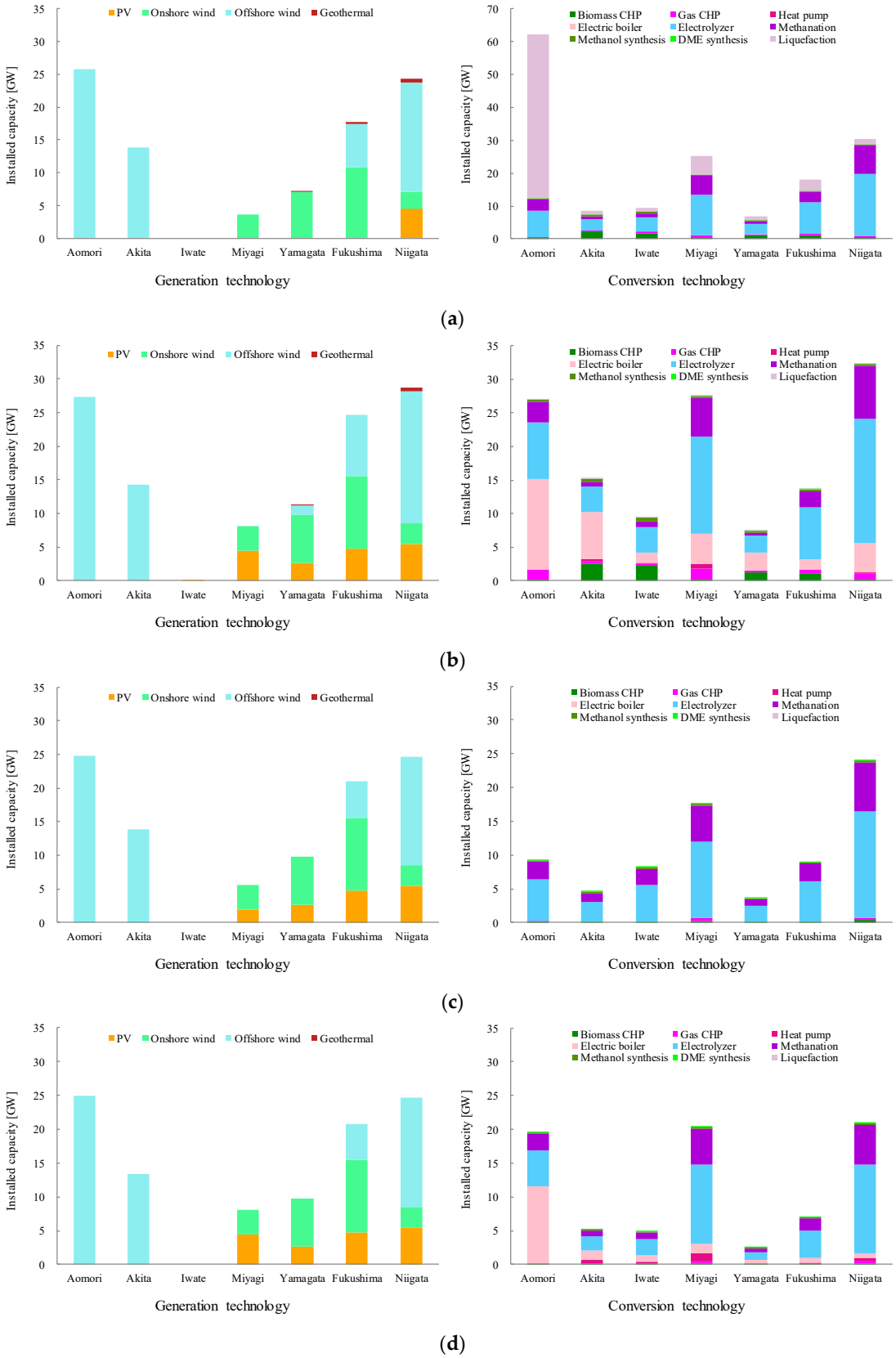

Figure 4. The optimal installed capacity of each technology. (**a**) All-BEV_IND scenario. (**b**) All-BEV_HD120 scenario. (**c**) All-BEV-V2G_IND scenario. (**d**) All-BEV-V2G_HD120 scenario.

The characteristics of the installed capacity of energy conversion technology differ depending on the DHS's utilization. In the All-BEV_IND scenario, many liquefaction facilities are installed in Aomori Prefecture. Since many offshore wind power generation plants are installed in Aomori Prefecture, much flexibility for intermittent power generation is required. The results suggest that P2G is the best option to resolve renewable energy's intermittency. Electrolyzers and fuel synthesizers account for the most installed capacity, particularly in Miyagi, Niigata, and Fukushima, where industrial fuel demand is high. In All-BEV_HD120 and All-BEV-V2G_HD120 scenarios, many EBs are installed in Aomori. This is because heat storage by EBs and HWTs is the cheapest option as flexibility for offshore wind power in Aomori. The electrolyzer and fuel synthesizer's installed capacity tends to be more prominent in the area where energy consumption in the industrial sector is high. In these scenarios, it can be confirmed that the installed capacity of the electrolyzer, fuel synthesizer, stationary battery, and HPT is reduced as compared with the All-BEV_IND scenario. Comparing the All-BEV_HD120 scenario with the All-BEV-V2G_HD120 scenario, the installed capacity of EB, CHP, electrolyzer, and fuel synthesizer are all reduced by the introduction of V2G.

The above results suggest that the use of DHS and V2G can reduce the installed capacity of P2G technologies such as electrolyzer and fuel synthesizers. This is because the flexibility offered by P2H and V2G for electricity networks makes the operations of P2G technologies effective. Figure 5 shows the duration curves of (a) electrolyzer and (b) methane synthesizer. The vertical axis intercept corresponds with the technology's installed capacity in these figures. When comparing All-BEV and All-BEV-V2G scenarios, the installed capacity of P2G technologies in All-BEV-V2G scenarios is reduced. The demand for hydrogen is almost equal between the All-BEV scenario and the All-BEV-V2G scenario, but the slope of the duration curve has become gentler with the introduction of V2G. This means that the electrolyzer's capacity factor (CF) has been improved, and the installed capacity has been reduced. When comparing IND scenarios with HD120 scenarios, it can be confirmed that the installed capacity of P2G technologies in HD120 scenarios has been reduced. The electrolyzer's capacity factor has improved from 0.42 in the All-BEV_IND scenario to 0.55 in the All-BEV_HD120 scenario.

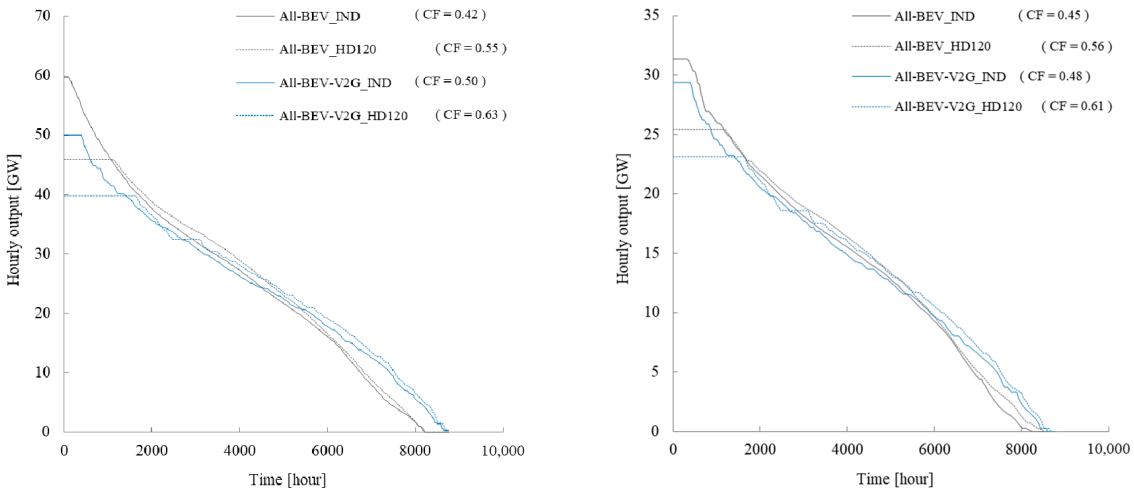

(**a**) (**b**)

Figure 5. Duration curves in each scenario. (**a**) Electrolyzer. (**b**) Methane synthesizer.

Furthermore, it has improved from 0.50 in the All-BEV-V2G_IND scenario to 0.63 in the All-BEV-V2G_HD120 scenario. As in the electrolyzer, the slope of the duration curves of the methane synthesizer becomes gentle due to the introduction of DHS and V2G.

In other words, the capacity factor has been improved, and DHS and V2G have reduced the installed capacity.

3.4. Hourly Energy Balances in the Sector-Coupled Energy System

Figure 6 shows the hourly electricity balances in each scenario. The electrolyzer and methane synthesizer's hourly operations are also shown in Figure 7. In the electricity balances of the All-BEV_IND scenario, fluctuations due to renewable energy can be adjusted by a stationary battery and the electrolyzer. As a result, the electrolyzer operation is selected as the primary option to offset the fluctuations. Therefore, the electrolyzer operation greatly depends on the fluctuation of renewable energy and is not stable, as shown in Figure 7a. Most of the produced hydrogen is used for methane synthesis, and the output of the synthesizer also fluctuates significantly, as shown in Figure 7b. In the electricity balances of the All-BEV_HD120 scenario, renewable energy fluctuations are adjusted by operating the stationary battery, electrolyzer, and electric boiler. Electric boilers operate at the peak of renewable energy supply. The operation of electrolyzer and methane synthesizer depends on renewable energy fluctuation. However, the outputs are partially suppressed by the peak cut effect of P2H, as shown in Figure 7a,b.

In the electricity balances of the All-BEV-V2G_IND scenario, fluctuations are adjusted by the operating electrolyzer and the use of V2G. The peak shift effect by V2G is working most of the time. Therefore, the electrolyzer and methane synthesizer operation in this scenario is more stable than that of the All-BEV_IND scenario, as shown in Figure 7a,b. In the electricity balance of the All-BEV-V2G_HD120 scenario, fluctuations of renewable energy are adjusted by operating the electrolyzer, the electric boiler, and V2G. The peak shift effect by V2G is working most of the time. Electric boilers are partially in operation at the peak of renewable energy supplies. The electrolyzer operation is leveled by the peak shift effect of V2G and the peak cut effect of P2H. The electrolyzer operation keeps an almost constant output, showing the peak cut and peak shift effects of P2H and V2G. Therefore, the output of the fuel synthesizer is also stable.

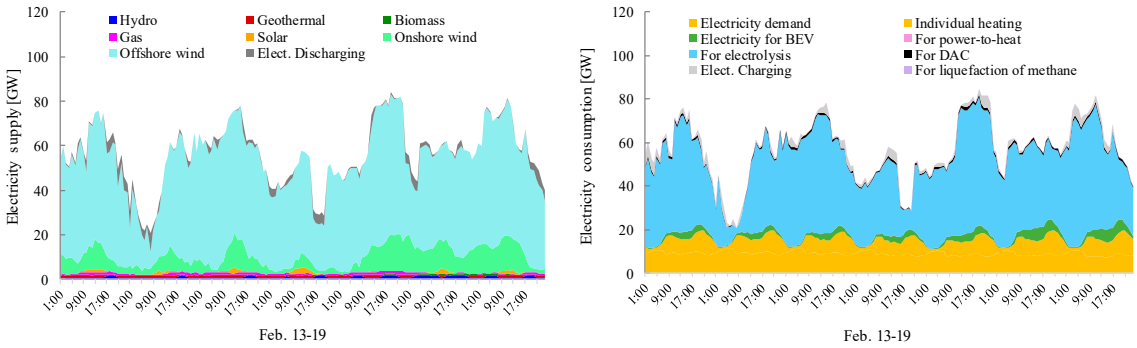

(**a**)

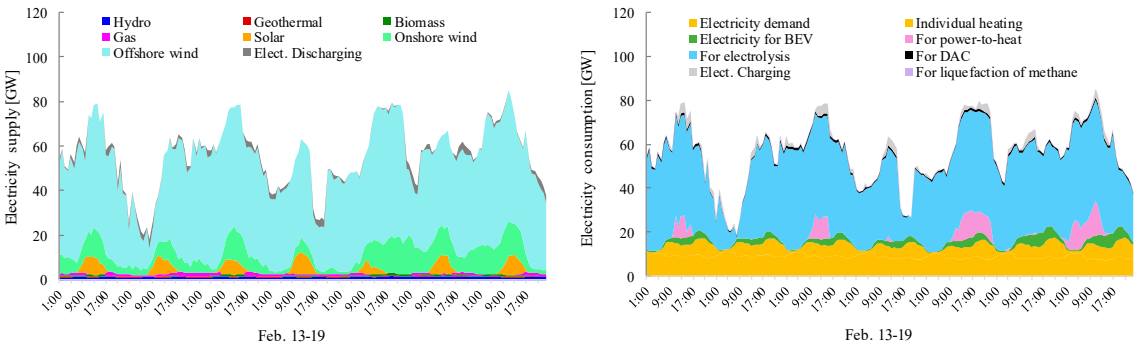

(**b**)

Figure 6. *Cont.*

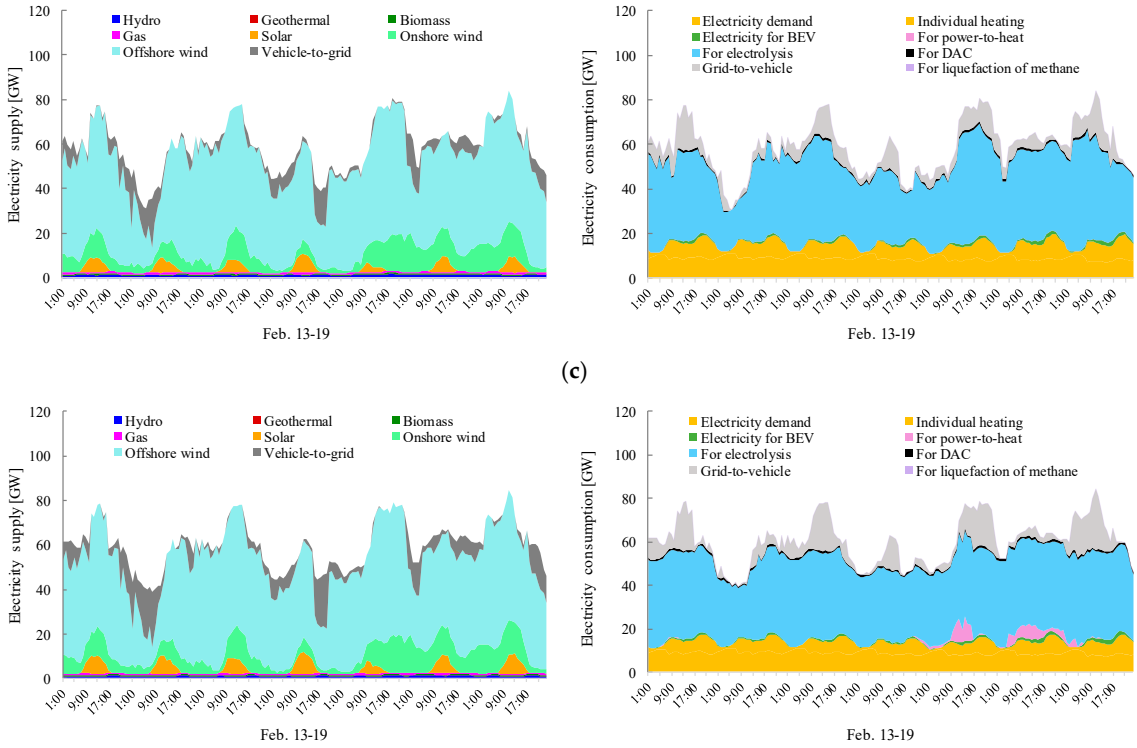

Figure 6. Hourly electricity balances in (**a**) All-BEV_IND scenario. (**b**) All-BEV_HD120 scenario. (**c**) A-BEV-V2G_IND scenario. (**d**) All-BEV-V2G_HD120 scenario.

Previous discussions suggest that the introduction of DHS and V2G could reduce the installed capacity of electrolyzer and fuel synthesizers, contributing to lower total annual system costs. When this is analyzed in detail, it becomes clear that the peak cut effect by P2H and the peak shift effect by V2G result in the leveling of the output of the electrolyzer and fuel synthesizer, which improves the capacity factor and reduces the installed capacity. In other words, this result suggests that the introduction of DHS and V2G not only enhances the flexibility of the electrical grid but also reduces the production cost of synthetic fuels for industry and transportation.

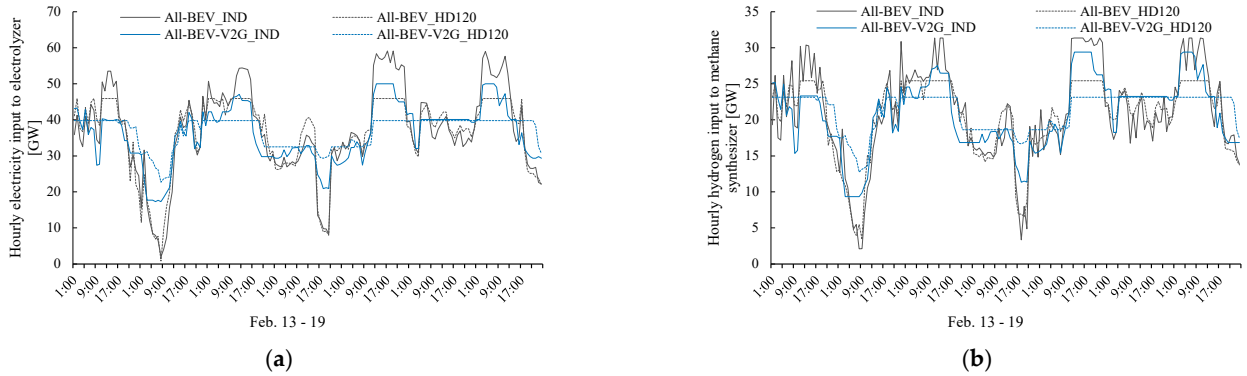

Figure 7. Hourly operation of Power-to-Gas technology in each scenario (**a**) Electrolyzer. (**b**) Methane synthesis.

3.5. Comparison with the Current Energy System

The sector-coupled energy system's characteristics are explained by comparing the current energy system with the energy flow diagrams. Figure 8 shows the energy flow diagram of (a) the current energy system and (b) the energy system considering the sector coupling designed by optimization. The system shown in (b) is based on a scenario in

which all vehicles in the transport sector are electric vehicles, of which passenger cars are used for V2G, and a district heating system is introduced into areas where the heat-demand density is 120 TJ/km^2 or more. The current energy flow diagram is based on statistical data estimates [27,28,30].

In the current energy system in the Tohoku region, TPES is 1495 PJ/year. The breakdown is 11.4 PJ for solar, 6.1 PJ for onshore wind, 37.5 PJ for hydro, 2.3 PJ for geothermal, 76.2 PJ for biomass, 343.5 PJ for coal, 335.1 PJ for natural gas, and 682.7 PJ for crude oil. Therefore, fossil fuels make up 91% of the total. The primary energy input to electricity generation is 589.9 PJ, with renewable energy accounting for 12.4% and fossil fuels accounting for 87.6%. In addition, 293.9 PJ, which accounts for 50% of the primary input energy, is lost at thermal power plants. The final energy consumption is 1270.7 PJ (electricity, 23.3%; biomass, 4.7%; and fossil fuels, 71.0%). The energy system's rejected energy is 293.9 PJ, and the system energy efficiency is 80.3%. The Tohoku region's current amount of CO_2 emissions was estimated to be 95.0 Mt-CO_2/year.

In the All-BEV-V2G_HD120 scenario, which is an example of a sector-coupled energy system, TPES is 1323.5 PJ/year. This is approximately 11.5% less than the current situation. The breakdown is 72.4 PJ for solar, 148.0 PJ for onshore wind, 938.1 PJ for offshore wind, 46.6 PJ for hydro, and 118.8 PJ for biomass. In the electricity generation sector, 1297.0 PJ of primary energy is supplied, generating 1237.9 PJ, approximately 4.2 times the current electricity generation. The electricity generation sector's rejected energy is 29.3 PJ (about 10% of the current level).

Final energy consumption decreases by 17.2% from the current level to 1052.7 PJ. This is due to the shift from internal combustion engine vehicles to electric vehicles and heat-demand electrification. The energy system's rejected energy is 300.7 PJ, and the system's energy efficiency is 77%. This is due to the energy loss during hydrogen production for fuel synthesis. Approximately 64% of the total electricity generation is consumed by the electrolyzer's operation, producing 489.2 PJ of hydrogen. The conversion loss is 224.1 PJ, and the waste heat recovery in the district heating system is 75.7 PJ. The energy demand of the CO_2 capture process by DAC is 140.4 PJ, accounting for about 12% of the total final energy consumption. In this study, it is assumed that synthetic fuels cover the fuel demand of the industrial sector, meaning a large amount of energy is lost when producing hydrogen for fuel synthesis. To improve energy system efficiency, reduction and electrification of fuel demand in the industrial sector are necessary.

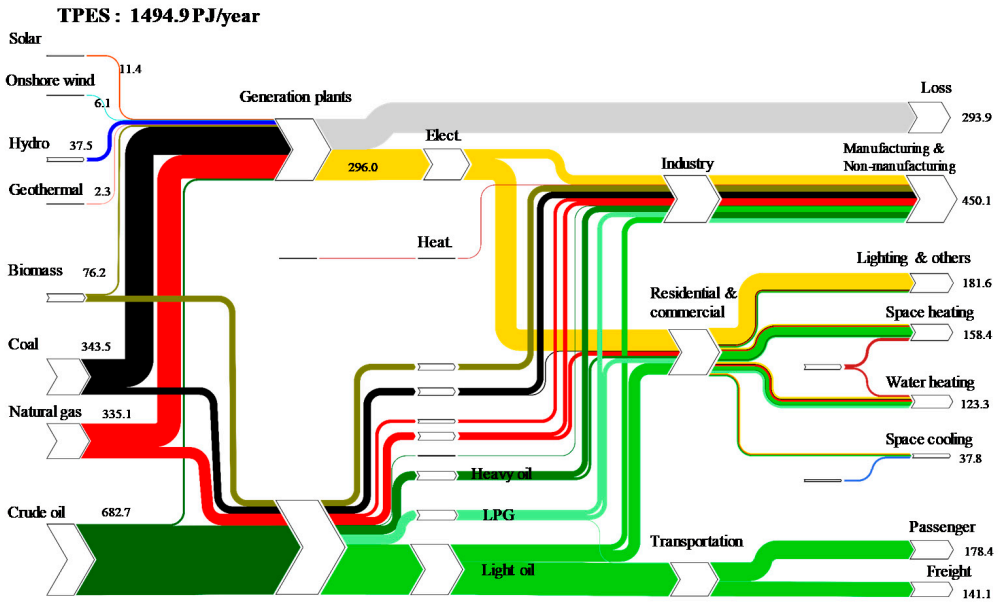

(**a**)

Figure 8. *Cont.*

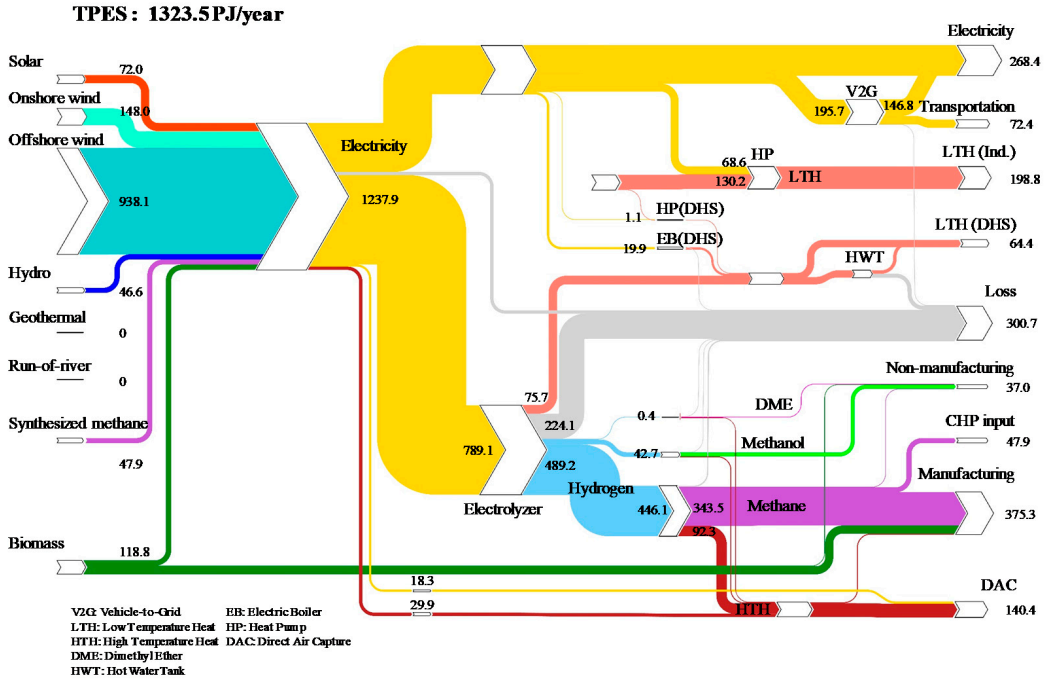

(**b**)

Figure 8. The energy flow chart in the Tohoku region. (**a**) Current energy system. (**b**) The sector-coupled energy system in the case of the All-BEV-V2G_HD120 scenario.

4. Discussion

4.1. Toward Implementation of the Sector-Coupled Energy System in Japan

In a sector-coupled energy system, the total primary energy supply decreases, but the amount of generation may be required to be about four times the current amount. In the Tohoku region, the share of renewable resources in the current generation is 12.4%. In order to realize this system, it is necessary to use 34 times as many renewable resources as is currently introduced. From the analysis of energy flow, it is confirmed that in the optimization model proposed in this study, the synthetic fuels supplied to the industrial sector have a considerable influence on the amount of power generation. The higher the share of energy consumption of the industrial sector in final energy consumption, the more power generation required. In the Tohoku region, the energy consumption of the industrial sector accounts for 35.4% of total final energy consumption, but in Japan, the energy consumption of the industrial sector accounts for 46.1% of total final energy consumption. In addition, the share of renewable resources in the current generation is 16% (2017). If this model is applied to Japan, simple calculations would not be possible, but it can be expected that it would be necessary to introduce more than 35 times the current amount of renewable energy. To verify the effects of sector coupling in Japan as a whole, an energy system model covering all regions is needed.

On the other hand, this study does not assume changes in energy demand. Energy demand is greatly affected by the economy and vital statistics. The Japanese population is already declining, and energy demand is also expected to decline. In addition, counter-measures against COVID-19 in 2020 have significantly changed our lifestyles, significantly impacting energy demand. If energy demand decreases, less renewable energy would be required; therefore, efforts to transform lifestyles on the demand side into sustainable ones are also important.

In addition, in sector-coupled energy systems, the total system cost may be more than double the current cost. To reduce the cost as much as possible, it is appropriate to promote electric vehicles in the transportation sector because fuel cell vehicles are inferior to electric vehicles in terms of overall energy efficiency. In addition, there is a possibility that the cost can be further reduced by utilizing the electric vehicle as a flexible carrier by V2G. It was confirmed that the district heating system also reduces the total system cost due to its flexibility through P2H. Japan is in a situation where it is difficult to secure the flexibility to the grid based on the "cross-border" concept that accommodates electricity between countries. Therefore, securing flexibility based on the "cross-sector" concept is the key to the mass introduction of renewable resources into the energy system. However, the penetration rate of district heating systems in Japan is low, and it is believed that they will not spread significantly in the future. Therefore, policy support is needed to promote district heating systems toward decarbonized society.

From the results of this study, the following suggestions were obtained regarding the roles required for each technology: First, regarding power generation technology, when there are few options for flexibility, it tends to be difficult to introduce PV generation. This is due to the characteristic that PV generation peaks during the day. The mass introduction of PV generation increases storage batteries and conversion technologies to cope with this peak, and the cost may increase accordingly. The results show that it is desirable to introduce a large amount of offshore wind power in areas with low LCOE in the target areas of this study. In the energy system where all couplings were taken into consideration, electric boiler, electric heat pump, and hot water tank in the district heating system have the effect of improving the capacity factor of electrolyzer in addition to the function as the flexibility to the electrical grid. Therefore, it was suggested that it might reduce the production cost of synthetic fuel. V2G also showed behavior that improves the capacity factor of the electrolyzer. In this study, P2G became a bottleneck for cost reduction. Therefore, when synthetic fuels are needed in areas where the share of industrial energy is high, it is better to avoid using P2G as the flexibility to the electrical grid. It is necessary to improve the capacity factor by making the output of the electrolyzer as stable as possible.

4.2. Possible Improvements

To consider reduction and electrification of fuel demands and direct use of hydrogen in the industrial sector, it is necessary to update the optimization model that includes the consumer's replacement cost of equipment. In the industrial sector, the chemical industry uses naphtha derived from crude oil distillation. Therefore, it is necessary to consider raw materials for chemical products not derived from crude oil. For example, there is synthesis from electrolyzed hydrogen and CO_2. There is a need for a model that considers reducing energy consumption due to improved energy efficiency through insulation and equipment replacement in the commercial and residential sectors. It is also desirable to consider waste heat from waste incineration plants in the district heating system. In the transportation sector, it is necessary to develop models that consider the recycling of batteries in BEV, the deterioration of batteries due to the use of V2G, the cost of power supply facilities to BEV, and the energy consumption of railways, ships, and aircraft. Moreover, it is necessary to evaluate the impact on V2G usage due to the decrease in the number of vehicles by car-sharing and ridesharing. In addition, the use of pumped storage power generation should be considered as flexible for variable renewable energy.

Moreover, in this study, it was not possible to analyze the technology that utilizes solar thermal. There was a lack of data on solar thermal in Japan, and reliable data could not be obtained; therefore, the model could not handle it. In the future, it will be necessary to prepare reliable data on solar heat and incorporate it into the optimization model. As with solar thermal, there is a lack of data on a load of refrigeration and cooling, meaning it is necessary to first prepare basic data and incorporate it into the optimization model.

Furthermore, there is a need to develop a model that considers cost reductions due to scale factors. Although this leads to a non-linear model, it is possible to estimate the introduction costs of electrolyzer and fuel synthesizer more precisely. In this study, we assumed that only electric power is the cross-border target. However, there is a possibility that a more efficient system can be designed by considering the cross-border of synthetic fuels.

In addition, in this model, it is a prerequisite that the introduction potential of renewable energy greatly exceeds the demand, which gives a feasible solution. For example, in Japan, it would be difficult to apply this model in areas where energy demand exceeds the introduction potential of renewable energy, such as around Tokyo and Osaka. Therefore, it is necessary to make it possible for the model to handle centralized power sources such as hydrogen power generation, ammonia power generation, and nuclear power generation. It is also necessary to extend this model to all regions of Japan by considering inter-regional transmission, reinforcement of transmission lines, and fuel transportation.

5. Conclusions

In this study, an optimization model of the energy system considering sector coupling has been developed and applied to the Tohoku region to reveal the required technologies and their costs and optimal operation in the sector-coupled energy system. As a result, the following findings are obtained.

- The total primary energy supply will decrease, but the amount of generation may be required to be about four times the current amount. In Japan, it can be expected that it would be necessary to introduce more than 35 times the current amount of renewable energy to realize decarbonization by renewable resources. The annual total system cost of the designed energy systems increases from 1.8 to 2.4 times the current level.
- The annual system cost of the scenario introducing district heating systems and using electric vehicles for V2G is minimal. As a result of the analysis of hourly energy balance, it becomes clear that the peak cut effect by P2H and the peak shift effect by V2G result in the leveling of the electrolyzer, and fuel synthesizer's output improves the capacity factor and reduces the introduction capacity. It is necessary to utilize electric vehicles by V2G and provide policy support for district heating systems to reduce costs.
- From the analysis of energy flow, it is confirmed that in the optimization model proposed in this study, the synthetic fuels supplied to the industrial sector have a considerable influence on the amount of power generation.
- There is a concern that the capacity of storage batteries and energy conversion technologies will increase to cope with the peak of PV. In areas where the industrial energy share is high, P2H and V2G may help reduce the cost of synthetic fuels. In addition, P2G should be mainly aimed at producing synthetic fuels, not flexibility.
- To reduce the amount of renewable energy required, it is necessary to reduce the energy demand in the industrial sector and electrify the energy demand. To reduce energy demand in the industrial sector, it is important to transform lifestyles that were not considered in this study into sustainable ones.
- For future research, it is important to incorporate more technologies, improve the model's accuracy with reliable data, and model the optimization on the demand side. It is also required to apply the model to all regions of Japan.

Author Contributions: Conceptualization, T.N. and N.N.; methodology, N.N.; software, N.N.; validation, N.N.; formal analysis, N.N.; investigation, N.N.; resources, N.N.; data curation, N.N.; writing—original draft preparation, N.N.; writing—review and editing, R.D. and T.N.; visualization, N.N.; supervision, R.D. and T.N.; project administration, T.N.; funding acquisition, T.N. All authors have read and agreed to the published version of the manuscript.

Funding: This research received no external funding.

Conflicts of Interest: The authors declare no conflict of interest.

Nomenclature

Sets

h	Hour
i	Link of transmission line
j	Other regions
n	Synthetic fuels (methane, methanol, DME)
t	Technology
$tc \in t$	Conversion technology
$tg \in t$	Generation technology
r	Region

Indices

$C^{CAPEX\&OPEX}$	Total capital and O&M costs (million JPY/year)
C^{carbon}	Total carbon capture costs (million JPY/year)
$C^{liq.}$	Total costs for methane liquefaction (million JPY/year)
C^{total}	Total annual system costs (million JPY/year)
$C^{trans.}$	Total transmission costs (million JPY/year)
$CC_{bio.}$, CC_{gas}, CC_{DAC}	The total amount of captured CO_2 (t-CO_2/year)
$pes^{bioCHP}_{bio.}$	Primary energy supply to CHP plants by woody biomass (GW)
$pes^{gasCHP}_{CH_4}$	Primary energy supply to CHP plants by methane (GW)
$Sto^{battery}_{elect.}$, $Sto^{bev}_{elect.}$	The amount of electricity stored in batteries (GWh)
$Sto^{HPT}_{H_2}$	The amount of hydrogen stored in high-pressure tanks (GWh)
Sto^{HWT}_{lth}	The amount of low-temperature heat stored in hot water tanks (GWh)
$Sto^{tank}_{CH_4(g)}$, $Sto^{tank}_{CH_4(l)}$.	The amount of methane stored in gas and liquid state (GWh)
Sto^{tank}_{n}	The amount of synthetic fuel stored in fuels tanks (GWh)
$Sto_{bio.}$	Woody biomass stock (GWh)
Sto_{CO_2}	The amount of CO_2 stored in tanks (t-CO_2)
$V2GCap$	Total allowed maximum vehicle-to-grid outputs (GW)

Parameters

A	Photovoltaic panel area (m^2/kW)
$c^{overnight}_{t}$	Overnight capital cost (million JPY/GW)
$Cap_{trs.}$	Transmission line capacity (GW)
$cap_{vbattery}$	The storage capacity of a battery in a vehicle (GWh/vehicle)
cd_n	CO_2 demands for fuels synthesis (t-CO_2/$GW_{hydrogen}$)
$cef_{bio.}$, cef_{CH_4}	The carbon emission factor of woody biomass and methane (t-CO_2/GWh)
CRF_t	Capital recovery factor (-)
$dmd^{manuf.}$	Annual fuels demand in the manufacturing industry (GWh)
$dmd^{nmanuf.}$	Annual fuels demand in the non-manufacturing industry (GWh)
$dmd^{transport.}_{elect.}$	Electricity consumption by BEV driving (GW)
$dmd_{elect.}$	Hourly electricity demand (GW)
dmd_{H_2}	Hourly hydrogen demand (GW)
dmd_{lth}	Hourly low-temperature heat demand (GW)
$DoD^{battery}$	Desirable depth of discharge for stationary battery (-)
$er^{DAC}_{elect.}$,	Electricity consumption for DAC (GWh/t-CO_2)
er^{DAC}_{hth}	High-temperature heat consumption for DAC (GWh/t-CO_2)
$er^{liq.}_{elect.}$	Electricity consumption from methane liquefaction (GWh/GWh)
I	Interest rate (-)
$Life_t$	A lifetime of technology (year)
$N_{vehicle}$	The number of vehicles (vehicle)
op_{tg}	The hourly output from renewables' generation technology (GW/GW)
$or^{battery}$	Output ratio to battery capacity (-)
p	Percentage of traveling vehicles (-)
$Pot_{bio.}$	Annual utilization potential of woody biomass (GWh)
Pot_{tg}	Installation potential of renewables' generation (GW)
rad	Solar radiation (MJ/m^2/h)
$SoC_{btm.}$, SoC_{up}	Desirable state of charge for battery in BEV (-)
$uc^{CAPEX\&OPEX}_{t}$	Unit capital and O&M cost of technology t (million JPY/GW)
$uc^{capital}_{t}$	The annualized unit cost of capital (million JPY/GW/year)
$uc^{cc}_{bio.}$, uc^{cc}_{DAC}, uc^{cc}_{gas}	The unit cost of carbon capture from CHP plants and DAC (million JPY/t-CO_2)
uc^{fuel}_{t}	The annualized unit cost of fuel (million JPY/GW/year)
$uc^{liq.}$	Unit cost for methane liquefaction (million JPY/GWh)
$uc^{O\&M}_{t}$	The annualized unit cost of capital, O&M, and fuel (million JPY/GW/year)
$uc^{trans.}$	The unit cost of electricity transmission (million JPY/GWh)
α	The available daily factor of vehicles (-)
β	Average trips per vehicle (-)
γ	Vehicle participation rate in V2G (-)
ζ^{bioCHP}, ζ^{gasCHP}	Specific electrical power loss for CHP (-)
η^{t}	Energy conversion efficiency (-)
$\eta^{bioCHP}_{elect.}$, $\eta^{gasCHP}_{elect,}$	Electrical efficiency of CHP plants (-)

$\eta^{battery}$	The efficiency of battery storage (-)
$\eta^{cc}_{bio.}$, $\eta^{cc}_{CH_4}$	Carbon capture efficiency in CHP plants (-)
η^{HEX}	Heat exchange efficiency (-)
η^{HWT}	The efficiency of hot water tank storage (-)
η^{hr}	The efficiency of heat recovery from fuel synthesizers (-)
η_{panel}, η_{pc}	The efficiency of photovoltaic panel and power conditioner (-)
$\theta^{vbattery}$	Allowed maximum vehicle-to-grid outputs per vehicle (GW)
σ^{bioCHP}, σ^{gasCHP}	The power-to-heat ratio of CHP in back-pressure operation (-)
Decision variables	
$c^{tc}_{x\to y}$	Energy conversion from x into y by technology tc (GW)
Cap_t	The capacity of technology t (GW)
$chg_{elect.}$,	Electricity charging to stationary batteries (GW)
chg_{lth}	Low-temperature heat charging to hot water tanks (GW)
dac	CO_2 captured by DAC (t-CO_2)
$hr^{ELZ.}$	Heat recovery from electrolyzer (GW)
hr^{FC}	Heat recovery from fuel cell (GW)
liq_{CH_4}	The amount of liquefied methane (GW)
$sup^{manuf.}_{n}$	Synthetic fuels supply to (non)manufacturing industry (GW)
$sup^{manuf.}_{hth}$	High-temperature heat supply to manufacturing industry (GW)
trs	The amount of electricity transmitted between regions (GW)
$v2g_{elect.}$	Electricity discharged from BEV to the electrical grid (GW)

References

1. Lund, H.; Østergaard, P.A.; Connolly, D.; Mathiesen, B.V. Smart Energy, and Smart Energy Systems. *Energy* **2017**, *137*, 556–565. [CrossRef]
2. Connolly, D.; Lund, H.; Mathiesen, B.V. Smart Energy Europe: The Technical and Economic Impact of One Potential 100% Renewable Energy Scenario for the European Union. *Renew. Sustain. Energy Rev.* **2016**, *60*, 1634–1653. [CrossRef]
3. Niemi, R.; Mikkola, J.; Lund, P.D. Urban Energy Systems with Smart Multi-Carrier Energy Networks and Renewable Energy Generation. *Renew. Energy* **2012**, *48*, 524–536. [CrossRef]
4. Thellufsen, J.Z.; Lund, H. Cross-Border versus Cross-Sector Interconnectivity in Renewable Energy Systems. *Energy* **2017**, *124*, 492–501. [CrossRef]
5. Syranidou, C.; Linssen, J.; Stolten, D.; Robinius, M. Integration of Large-Scale Variable Renewable Energy Sources into the Future European Power System: On the Curtailment Challenge. *Energies* **2020**, *13*, 5490. [CrossRef]
6. Tremel, A.; Wasserscheid, P.; Baldauf, M.; Hammer, T. Techno-Economic Analysis for the Synthesis of Liquid and Gaseous Fuels Based on Hydrogen Production via Electrolysis. *Int. J. Hydrogen Energy* **2015**, *40*, 11457–11464. [CrossRef]
7. Götz, M.; Lefebvre, J.; Mörs, F.; McDaniel Koch, A.; Graf, F.; Bajohr, S.; Reimert, R.; Kolb, T. Renewable Power-to-Gas: A Technological and Economic Review. *Renew. Energy* **2016**, *85*, 1371–1390. [CrossRef]
8. Guilera, J.; Ramon Morante, J.; Andreu, T. Economic Viability of SNG Production from Power and CO_2. *Energy Convers. Manag.* **2018**, *162*, 218–224. [CrossRef]
9. Ikäheimo, J.; Pursiheimo, E.; Kiviluoma, J.; Holttinen, H. Role of Power to Liquids and Biomass to Liquids in a Nearly Renewable Energy System. *IET Renew. Power Gener.* **2019**, *13*, 1179–1189. [CrossRef]
10. Varone, A.; Ferrari, M. Power to Liquid and Power to Gas: An Option for the German Energiewende. *Renew. Sustain. Energy Rev.* **2015**, *45*, 207–218. [CrossRef]
11. Blanco, H.; Nijs, W.; Ruf, J.; Faaij, A. Potential of Power-to-Methane in the EU Energy Transition to a Low Carbon System Using Cost Optimization. *Appl. Energy* **2018**, *232*, 323–340. [CrossRef]
12. Nastasi, B.; Mazzoni, S.; Groppi, D.; Romagnoli, A.; Astiaso Garcia, D. Solar power-to-gas application to an island energy system. *Renew. Energy* **2021**, *164*, 1005–1016. [CrossRef]
13. Bloess, A. Impacts of Heat Sector Transformation on Germany's Power System through Increased Use of Power-to-Heat. *Appl. Energy* **2019**, *239*, 560–580. [CrossRef]
14. Obara, S.; Ito, Y.; Okada, M. Electric and Heat Power Supply Network of Hokkaido in Consideration of the Leveling Effect by a Wide-Area Interconnection of Wind-Farm and Solar-Farm. *Trans. JSME* **2017**, *83*. [CrossRef]
15. Ashfaq, A.; Kamali, Z.H.; Agha, M.H.; Arshid, H. Heat Coupling of the Pan-European vs. Regional Electrical Grid with Excess Renewable Energy. *Energy* **2017**, *122*, 363–377. [CrossRef]
16. Taljegard, M.; Göransson, L.; Odenberger, M.; Johnsson, F. Impacts of Electric Vehicles on the Electricity Generation Portfolio—A Scandinavian-German Case Study. *Appl. Energy* **2019**, *235*, 1637–1650. [CrossRef]
17. Child, M.; Nordling, A.; Breyer, C. The Impacts of High V2G Participation in a 100% Renewable Åland Energy System. *Energies* **2018**, *11*, 2206. [CrossRef]
18. Brown, T.; Schlachtberger, D.; Kies, A.; Schramm, S.; Greiner, M. Synergies of Sector Coupling and Transmission Reinforcement in a Cost-Optimised, Highly Renewable European Energy System. *Energy* **2018**, *160*, 720–739. [CrossRef]
19. Bailera, M.; Lisbona, P.; Peña, B.; Romeo, L.M. A review on CO_2 mitigation in the iron and steel industry through power to X processes. *J. CO_2 Util.* **2021**, *46*. [CrossRef]

20. IEA. *World Energy Balances 2018*; IEA: Paris, France, 2018. [CrossRef]
21. Takita, Y.; Furubayashi, T.; Nakata, T. Development and Analysis of an Energy Flow Considering Renewable Energy Potential. *Trans. JSME* **2015**, *81*. [CrossRef]
22. Lehner, M.; Tichler, R.; Steinmüller, H.; Koppe, M. *Power-to-Gas: Technology and Business Models*; Springer: Berlin/Heidelberg, Germany, 2014. [CrossRef]
23. Lund, H.; Werner, S.; Wiltshire, R.; Svendsen, S.; Thorsen, J.E.; Hvelplund, F.; Mathiesen, B.V. 4th Generation District Heating (4GDH). Integrating Smart Thermal Grids into Future Sustainable Energy Systems. *Energy* **2014**, *68*, 1–11. [CrossRef]
24. Tohoku Electric Power Co., Inc. Power System Diagram (Primary System). Available online: https://www.tohoku-epco.co.jp/jiyuka/04/5001.pdf (accessed on 4 February 2020).
25. Tohoku Electric Power Co., Inc. Normal Operation Capacity Used for Studying System Access of Trunk Transmission Lines in the Region. Available online: https://www.tohoku-epco.co.jp/jiyuka/04/02.pdf (accessed on 4 February 2020).
26. Investigation Committee on Electricity Transmission Fee. Changes of Electric Charge and Transmission Fee. Available online: https://www.cao.go.jp/consumer/content/20180105_20160726_takuso_toshin_betu_shiryou.pdf (accessed on 4 February 2020).
27. Tohoku Electric Power Co., Inc. Download Past Actual Data. Available online: http://setsuden.tohoku-epco.co.jp/download.html (accessed on 4 February 2020).
28. Ministry of Economy, Trade and Industry. Energy Consumption Statistics by Prefecture. Available online: https://www.enecho.meti.go.jp/statistics/energy_consumption/ec002/ (accessed on 4 February 2020).
29. E-Stat. Population Census. Available online: https://www.e-stat.go.jp/gis/statmap-search?page=1&type=1&toukeiCode=00200521 (accessed on 4 February 2020).
30. Envirolife Research Institute Inc. *Annual Household Energy Statistics (2017)*; Envirolife Research Institute Inc.: Tokyo, Japan, 2019.
31. Fujii, S.; Furubayashi, T.; Nakata, T. Design and Analysis of District Heating Systems Utilizing Excess Heat in Japan. *Energies* **2019**, *12*, 1201. [CrossRef]
32. Okumura, K.; Ikaga, T.; Kawakubo, S. Development of the Database for Stock and Flow Floor Area of Non-Residential Buildings Classified by Building Use Type and Area. *AIJ J. Technol. Des.* **2012**, *18*, 275–280. [CrossRef]
33. Japan District Heating & Cooling Association. *Handbook of District Heating and Cooling Technologies*, 4th ed.; Japan District Heating & Cooling Association: Tokyo, Japan, 2013.
34. Werner, S. District Heating and Cooling. In *Reference Module in Earth Systems and Environmental Sciences*; Elsevier: Amsterdam, The Netherlands, 2013. [CrossRef]
35. Ministry of Land, Infrastructure, Transport and Tourism. Automotive Fuel Consumption Survey. Available online: https://www.mlit.go.jp/k-toukei/nenryousyouhiryou.html (accessed on 4 February 2020).
36. Uchida, T.; Furubayashi, T.; Nakata, T. Well-to-Wheel Analysis and a Feasibility Study of Fuel Cell Vehicles in the Passenger Transportation Sector. *Trans. JSME* **2019**, *85*. [CrossRef]
37. National Renewable Energy Laboratory. *Fuel Cell Buses in U.S. Transit Fleets: Current Status 2018*; National Renewable Energy Laboratory: Denver, CO, USA, 2018.
38. Lee, D.Y.; Elgowainy, A.; Kotz, A.; Vijayagopal, R.; Marcinkoski, J. Life-Cycle Implications of Hydrogen Fuel Cell Electric Vehicle Technology for Medium- and Heavy-Duty Trucks. *J. Power Sources* **2018**, *393*, 217–229. [CrossRef]
39. GoGoEV. Total Charging Record Information. Available online: https://ev.gogo.gs/special/using_report/ (accessed on 4 February 2020).
40. Ministry of the Environment. The Study of Basic Zoning Information on Renewable Energy. Available online: https://www.env.go.jp/earth/ondanka/rep/ (accessed on 4 February 2020).
41. Japan Meteorological Agency. Download Past Weather Data. Available online: https://www.data.jma.go.jp/gmd/risk/obsdl/ (accessed on 4 February 2020).
42. KYOCERA Corporation. Catalog of Solar Power Generating Systems for Public/Industrial Use. Available online: https://www.kyocera.co.jp/solar/support/download/uploads/catalog_kyocera_solar_business_1.pdf (accessed on 17 February 2020).
43. Japan Oceanographic Data Center. Coastal Maritime Meteorology Data. Available online: https://www.jodc.go.jp/jodcweb/JDOSS/fixed_wave_station_code_j.html (accessed on 4 February 2020).
44. Forestry Agency. Current Status of Forest Resources. Available online: http://www.rinya.maff.go.jp/j/keikaku/genkyou/index1.html (accessed on 4 February 2020).
45. Brynolf, S.; Taljegard, M.; Grahn, M.; Hansson, J. Electrofuels for the Transport Sector: A Review of Production Costs. *Renew. Sustain. Energy Rev.* **2018**, *81*, 1887–1905. [CrossRef]
46. Power Generation Cost Verification Working Group. Report on Verification of Power Generation Costs to the Long-Term Energy Supply and Demand Outlook Subcommittee. Available online: https://www.enecho.meti.go.jp/committee/council/basic_policy_subcommittee/mitoshi/cost_wg/pdf/cost_wg_02.pdf (accessed on 17 February 2020).
47. Dahl, M.; Brun, A.; Andresen, G.B. Cost Sensitivity of Optimal Sector-Coupled District Heating Production Systems. *Energy* **2019**, *166*, 624–636. [CrossRef]
48. Rubin, E.S.; Davison, J.E.; Herzog, H.J. The Cost of CO_2 Capture and Storage. *Int. J. Greenh. Gas Control* **2015**, *40*, 378–400. [CrossRef]
49. Zakeri, B.; Syri, S. Electrical Energy Storage Systems: A Comparative Life Cycle Cost Analysis. *Renew. Sustain. Energy Rev.* **2015**, *42*, 569–596. [CrossRef]

50. David, A.; Mathiesen, B.V.; Averfalk, H.; Werner, S.; Lund, H. Heat Roadmap Europe: Large-Scale Electric Heat Pumps in District Heating Systems. *Energies* **2017**, *10*, 578. [CrossRef]
51. Schmidt, O.; Gambhir, A.; Staffell, I.; Hawkes, A.; Nelson, J.; Few, S. Future Cost and Performance of Water Electrolysis: An Expert Elicitation Study. *Int. J. Hydrogen Energy* **2017**, *42*, 30470–30492. [CrossRef]
52. Energy Technology Systems Analysis Program (ETSAP). *Technology Brief P03: Oil and Natural Gas Logistics*; International Energy Agency (IEA): Paris, France, 2011; pp. 1–7.
53. Fasihi, M.; Bogdanov, D.; Breyer, C. Long-Term Hydrocarbon Trade Options for Maghreb Core Region and Europe—Renewable Energy Based Synthetic Fuels for a Net Zero Emissions World. *Sustainability* **2016**, *3*, 306. [CrossRef]
54. Staffell, I.; Brett, D.; Brandon, N.; Hawkes, A. A Review of Domestic Heat Pumps. *Energy Environ. Sci.* **2012**, *5*, 9291–9306. [CrossRef]
55. NISSAN. NISSAN LEAF Web Catalog. Available online: https://www3.nissan.co.jp/content/dam/Nissan/jp/vehicles/leaf/1912/pdf/leaf_1912_specsheet.pdf (accessed on 4 February 2020).
56. Tan, K.M.; Ramachandaramurthy, V.K.; Yong, J.Y. Integration of Electric Vehicles in Smart Grid: A Review on Vehicle to Grid Technologies and Optimization Techniques. *Renew. Sustain. Energy Rev.* **2016**, *53*, 720–732. [CrossRef]
57. EPA. Direct Emissions from Stationary Combustion Sources. *Energy Econ.* **2008**, *34*, 1580–1588. [CrossRef]
58. *The Institute of Energy Economics, Japan, Japanese Version of Handbook of Japan's & World Energy & Economic Statistics*; The Institute of Energy Economics: Tokyo, Japan, 2019.
59. Ministry of Economy, Trade and Industry. Petroleum Equipment Survey. Available online: https://www.enecho.meti.go.jp/statistics/petroleum_and_lpgas/pl006/ (accessed on 4 February 2020).
60. Ministry of Economy, Trade and Industry. *Gas Business Annual Report*; Ministry of Economy, Trade and Industry: Tokyo, Japan, 2018.
61. Persson, U.; Wiechers, E.; Möller, B.; Werner, S. Heat Roadmap Europe: Heat Distribution Costs. *Energy* **2019**, *176*, 604–622. [CrossRef]